MEDDELANDE FRÅN
GEODETISKA INSTITUTIONEN VID UPPSALA UNIVERSITET

Communication from the
Geodetic Institute Uppsala University
No. 15

TIDAL STUDIES FOR THE AEGEAN SEA

Doctoral dissertation

by

Evangelos Livieratos

UPPSALA 1976

Digitized by the Internet Archive
in 2026

https://archive.org/details/IA41548926_0021

TIDAL STUDIES FOR THE AEGEAN SEA

by

E. Livieratos*, Dipl. Eng., Dr.Eng.

Faculty of Rural and Surveying Engineering
National Technical University
Athens, Greece,

and

Institute of Geodesy and Geophysics
University of Trieste
Trieste, Italy.

* at present: "Alexander von Humboldt-Stiftung" fellow; Munich, Federal Republic of Germany.

To

Mariangela

UNIV.
LEIDEN
BIBL.

PREFACE

Purpose of this work is to start the study and a discussion on the tidal behaviour of the Aegean sea, considered as a partially closed basin, by solving numerically the corresponding hydrodynamic equations.

From the very beginning we had to face two a-priori difficulties:

a. The Aegean's nature itself, which forms a very special case of a partially closed basin, -compared to other basins like the Adriatic, the Baltic, the Black Sea etc.-, because of its irregular shape, its two openings at the south, its very anomalous bathymetry and because of the presence of a large number of islands within the basin.

b. The lack of previous sufficient information concerning harmonic constants at coastal sites as well as the non-existance of a previous similar solution for the Aegean tides.

So we tried to attack the problem by using available and usable actual data and making an extensive use of the computer, in order to study the response of several models of

the Aegean basin under a variety of input conditions.

The whole paper is organized in the following way: At the first chapter a general discussion is given describing in a simple way the induced and independent oscillations within partially closed basins; the second chapter deals with the Aegean sea, its connection with the Mediterranean sea, its topography and with the up to now existing tidal information; chapter three deals with the analysis of tidal registrations from two sites of the Aegean sea, using the spectral analysis method; in chapter four the theory of the numerical solution of the hydrodynamic equations is given followed by a detailed application on the Aegean in chapter five. Finally using the M2 semidiurnal solution, we give an order of magnitude of the loading effects on the Dionysos Satellite Tracking Station, for both the N-S and W-E components of the Newtonian effect. The conclusions and the proposals at the end outline the future work which has to be carried out in order to exaust the study of the Aegean tides.

With frequent references to Bibliography we tried to keep the subject of the paper at its main scope.

Basic terminology and properties on time series analysis, matrix calculus, hydrodynamics etc. are considered as known. For the symbols we tried to keep the symbolism followed by the international litterature, but giving always within the text the specific meaning of the symbol.
In some few cases it was impossible to avoid the use of the same symbol in order to describe a different quantity, but from the text comes always the evident meaning.

The lenghty computer output results are summarized in figures and Tables and the computer programmes used, all in FORTRAN IV, are already classified at the computer library of the Istituto di Geodesia e Geofisica, University of Trieste, Italy, where the present work has been carried out.

Acknowledgements

This work has been carried out at the Institute of Geodesy and Geophysics, University of Trieste, Italy, (January to June 1976), as a result of fruitful discussions with Prof. Maria Zadro, University of Trieste, during our stay with the Geodetic Institute of the Uppsala University, Sweden, (January to December 1975), guests of Prof. Erik Tengström.

I am indebted to Prof. M. Zadro for her advise, help and continuous encouragement to deal with geodynamical problems, as well as for her valuable comments and suggestions throughout this work.
Thanks are also due to colleagues and the staff of the Institute of Geodesy and Geophysics, University of Trieste, for their help.

The substancial support of Prof. E. Tengström, University of Uppsala, his encouragement, help and the great hospitality he offered me during my stay in Sweden, is gratefully acknowledged.

The active help of Prof. G. Veis, NTU of Athens, as well as the support of the Hydrographic Service of the Hellenic Navy by providing tidal data, is highly appreciated.

The present work was financialy supported by grants from the "Consiglio Nazionale delle Ricerche" and the "Commissione Geodetica Italiana", Italy.
An "Alexander von Humboldt-Stiftung" fellowship for research at the Federal Republic of Germany, (July to December 1976), allowed the conclusion and the presentation of this paper.

Contents

	Page
PREFACE	1
Acknowledgements	4
Contents	5
List of Figures	7
List of Tables	8
Abbreviations	8
1. INTRODUCTION	9
1.1. Induced and independent oscillations.	10
1.2. The process for the Aegean Sea.	12
2. THE AEGEAN SEA	14
2.1. The connection with the Mediterranean tides.	14
2.2. The topography of the Aegean.	16
2.3. Existing information.	21
3. ANALYSIS OF DATA	26
3.1. The general equation.	26
3.2. The method of analysis.	27
3.3. Analysis for Kavala and Heraklion.	31
3.4. The results.	34
4. SOLUTION OF THE HYDRODYNAMIC EQUATIONS	45
4.1. The acceleration of the water particles.	45
4.2. The gradient of pressure.	48
4.3. The friction.	49
4.4. The Coriolis force.	49

4.5. The continuity condition. 52
4.6. Application to natural basins. 53
4.7. The formation of the grid. 57
4.8. On the matrix analysis of the system. 62
4.9. Impulse response; eigenfrequencies. 66

5. NUMERICAL SOLUTION FOR THE AEGEAN SEA 71
5.1. The modeling. 71
5.2. The solution. 75
5.3. M2 wave propagation. 79
5.4. The transfer functions. 81
5.5. The eigenvalues. 88
5.6. Discussion on the results. 89

6. THE LOADING EFFECTS 100
6.1. The general theory. 101
6.2. M2 loading effects on the Dionysos Satellite Tracking Station. 102

7. CONCLUSIONS AND PROPOSALS 107

References 111
Curriculum vitae 117

List of Figures

		Page
Fig. 1	The Aegean sea within the Mediterranean.	15
Fig. 2	K1,P1 Mediterranean tides.	17
Fig. 3	M2 Mediterranean tides.	18
Fig. 4	The Aegean Bathymetry.	20
Fig. 5	Propagation of the max observed tidal amplitudes /Aegean sea.	23
Fig. 6	Propagation of the average observed tidal amplitudes /Aegean sea.	24
Fig. 7	Establishment of ports/Aegean sea.	25
Fig. 8	Tidal-stations' sites /Aegean sea.	28
Fig. 9	Location of the tide-gauges within the ports of Kavala and Heraklion.	30
Fig. 10	Logs of spectral amplitudes, Kavala.	41
Fig. 11	Logs of spectral amplitudes, Heraklion.	44
Fig. 12	5-points cross type descretization design.	58
Fig. 13	2-central points descretization design.	58
Fig. 14	MOD10 and MOD30 /Aegean sea.	72
Fig. 15	MOD30; profiles, test impulses.	77
Fig. 16	M2 wave propagation/Aegean sea.	80
Fig. 17	Transfer function profiles.	82
Fig. 18	Test phase-distribution; case 1.	90
Fig. 19	Test phase-distribution; case 2.	91
Fig. 20	Test phase-distribution; case 3.	92
Fig. 21	Test phase-distribution; case 4.	93
Fig. 22	Test phase-distribution; case 5.	94
Fig. 23	Distribution of the Newtonian effect for amplitude concerning a cm^2 water area.	104

List of Tables

		Page
Tab. 1	Monthly amplitudes for Kavala.	39
Tab. 2	Diurnal and semidiurnal amlitudes for Heraklion (3 months analysis).	40
Tab. 3	Amplitudes and corresponding phases for Kavala.	40

Abbreviations

LTE	Laplace Tidal Equation
NAB	North Aegean Basin
SAB	South Aegean Basin
KAV	Kavala
HER	Heraklion
OGS	Osservatorio Geofisico Sperimentale, Trieste.
GMT	Grenwich Mean Time
CIO	Conventional International Origin.
IPMS	International Polar Motion Service
MOD10	Grid model of 10x10 prime rectangles
MOD30	Grid model of 30x30 prime rectangles
CINECA	Centro Italia Nord Est Calcolo Automatico.
N,S,W,E	North, South, West, East (also combined).

1. INTRODUCTION

The study of the sea tides' behaviour is a very important tool when analyzing several oceanographic, geophysical, geodetic or in general geodynamical problems. For instance sea-current phenomena, dynamics of the oceanic water-flux, investigations on navigation problems, topics in dynamical geodesy -e.g. levelling-, loading effects, found always answers by treating the sea tidal effects. (For the associated hydrodynamical aspects see for instance the classical works by Lamb 1931 and Defant 1961).

Knowing a-priori the bathymetry of the oceans or smaller closed basins as well as the induced tides, we could study the tidal wave distributions, the tidal wave propagation or the response of the oceans to tidal forces by solving systems of equations which are derived by the Laplace Tidal Equations, LTE, (see for instance Hansen 1940, Defant 1961, Hendershott 1973). If tidal harmonic constants for some points at the basin's coast and/or at the open sea, are given -derived by analyzing tidal observations- the system of the LTE is constrained providing better results. Here we have to recall the fact that in small closed basins

the astronomic tides are not influecing the solution.

The solution could be carried out either analytically in special model-cases where we could formulate the problem mathematicaly, which in fact is a difficult procedure in practice (Van Dantzing 1958, Van Dantzing and Lauwerier 1959) or numerically, which is actually the more realistic, reasonable and feasible way, (see for instance Hansen 1940, 1943, 1948, Bogdanov and Magarik 1967, 1969, Hendershott and Munk 1970, Baxa et al. 1970, Baxa et al. 1973, Platzman 1975, Bozzi Zadro 1976).

1.1. Induced and independent oscillations.

In this work we study the response of the Aegean sea to tidal forces, considered as a basin connected with the Mediterranean sea -which acts as a tide inducing sea- through the two openings western and eastern of Crete. In general, when natural basins are communicating with the open sea by one or more openings we have always induced

oscillations which depend on the amplitudes of the entering waves influenced as well by the hour angle, the declination and the parallax of the Moon and the Sun.
The imposed oscillations propagate progressively within the basin with a velocity which depends on the basin's depth considering as well the Coriolis force influences on the water particle's path and reflected at the coastal boundaries, turn propagating to the opposite way.
The conjunction of the original and the reflected waves results the observed water-particle displacement within the basin.

Apart from the presence of the induced oscillations of stationary character described above, we have the forced oscillations -independent tides- caused by the Moon-Sun tidal effects which combined with the induced ones plus several meteorological and seiches' effects, complicate the overall propagation of the tidal waves in a basin communicating to open seas, (Lamb 1931, discusses extensively the oscillations for a variety of models). For small basins the independent tides are almost negligible, compared with the induced ones.

For basins communicating with open seas, Theory and Practice coincide almost always (Tenani 1940), verifying the presence of stationary oscillations around a nodal axis -no vertical water movements- or an amphidromic point generated by the Coriolis effect which is a well known function of latitude.

1.2. The process for the Aegean sea.

From the above elementary description of the two types of oscillations within a basin communicating with the open sea, we could realize how interesting should be to investigate the response of the Aegean sea to tidal forces, considering its complicated shape, the presence of too many islands which reflect and/or filter the imposed waves in a non-uniform way, the existance of two openings to the Mediterranean sea and finally its anomalous bottom relief.

The investigation was based on the numerical solution of the hydrodynamic equations for the Aegean sea, for the semidiurnal tides, by modeling the basin using 10-prime

Mercator squares and interpolating depths obtained by the recent detailed bathymetric map of the Aegean, compiled by Morelli et al. 1975. Applying matrix analysis methods on a model of 30-prime Mercator squares, we discuss the impulse response of the sub-basins of the Aegean sea, between 3 and 24 hours-period, as well as its eigenfrequencies. The imposed M2 wave tidal harmonic constants at the openings of the Aegean, were obtained from the already existing Mediterranean solution (Baxa et al. 1973) constrained by tidal harmonic constants from some sites on the Aegean coasts given by Tenani 1940 and by the spectral analysis of tidal data from the ports of Kavala and Heraklion, included in this work.

A M2 tidal map is constracted followed by sensitivity analysis of the basin, to several input-values as well as the loading effects due to the M2 tidal waves, on the Dionysos Satellite Tracking Station, situated near the eastern coast of Attica.

2. THE AEGEAN SEA

The Aegean sea is one of the two independent basins of the Mediterranean -the other being the Adriatic sea-.
Its coastal boundaries are the eastern and northern Hellenic coasts, the western coast of Turkey and the northern coast of Crete,(Fig.1). Communicates with the Mediterranean by two openings, eastern and western of Crete. For diurnal tidal frequencies oscillates in a stationary mode around a traversal nodal line northern of the island of Lesos; the influence of the Coriolis force transforms the nodal line to an amphidromic node.

2.1. The connection with the Mediterranean tides.

The open sea influencing the Aegean basin is the Mediterranean which is an enlarged basin itself, oscillating as well in a stationary mode around three nodal points, as far as the semidiurnal tides are concerned. The W-Mediterranean (from Gibraltar to the Tunisian-Sicilian strait) oscillates around a nodal point between Algeria and the

Fig. 1. The Aeagen sea within the Mediterranean.

E-coast of Spain. The establishments of the ports are of about 9 hours at the Tyrrenian coast. The central Mediterranean has a nodal point at the Sicilian channel while the E-Mediterranean, which in fact influences in a substancial way the Aegean basin, oscillates around a nodal point passing southwestern of Crete; the establishments of the ports are of about 3 hours at the oriental Sicilian coast and of about 10 hours at the southrn coast of Asia Minor, (Tenani 1940). The phases and amplitudes of the Mediterranean are shown in Fig. 2 and Fig. 3 ,(Baxa et al. 1973).

2.2. The topography of the Aegean.

As we mentioned above the Aegean basin is connected with the Mediterranean by two openings: The eastern opening (E-opening) east of Crete, is twice wider than the western one (W-opening) west of Crete, thus should be considered as the more important one concerning the leading waves from the eastern Mediterranean.

The bottom relief of the Aegean is very anomalous, (Fig. 4) forming clearly two smaller basins: The North Aegean Basin

(see Baxa et al. 1973)

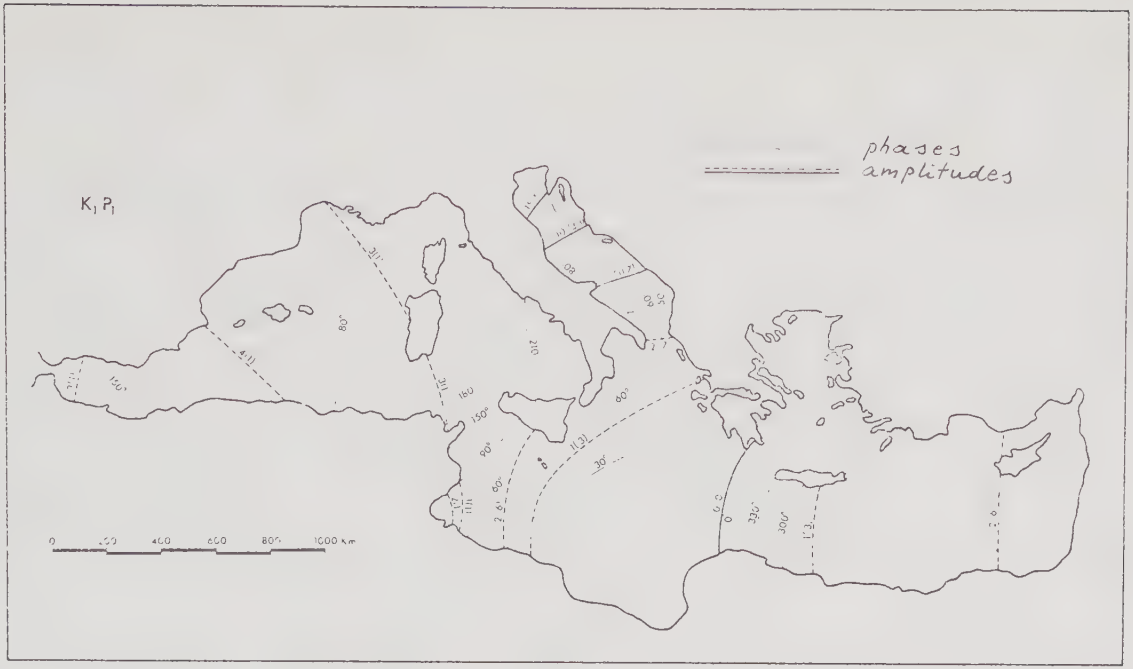

Fig. 2. K1, P1 Mediterranean tides.

(see Baxa et al. 1973)

Fig. 3. M2 Mediterranean tides.

(NAB) bordered at the N by the northern Hellenic coast and at the S by the Cycladic complex platform, plus the channel-type connection with the eastern Mediterranean. The depths of the central NAB are varying in general between 400 to 700 m, while the depths close to the coast are between few meters and 200 m; a deep trench running towards the NE direction, at the northern NAB, has varying depths between 800 and 1500 m; The depths of the Cycladic complex platform are not more than 200 m, while the channel-type southwestern NAB has depths between 500 and 3000 m, (close to the E-opening). In general we could say that the main NAB has an average depth of about 450 m.

The South Aegean Basin (SAB) bordered by the Cycladic block and Crete, connected with the Ionian and Adriatic seas, though is smaller than the NAB, it is in general deeper with an average depth of about 1000 m, but a notable depth of about 3000 m exists along the W-opening. In Fig. 4 the bottom topography of the Aegean was averaged by using 5-prime Mercator squares, based on the bathymetric map compiled by Morelli et al. 1975.

Fig. 4. The Aegean Bathymetry.

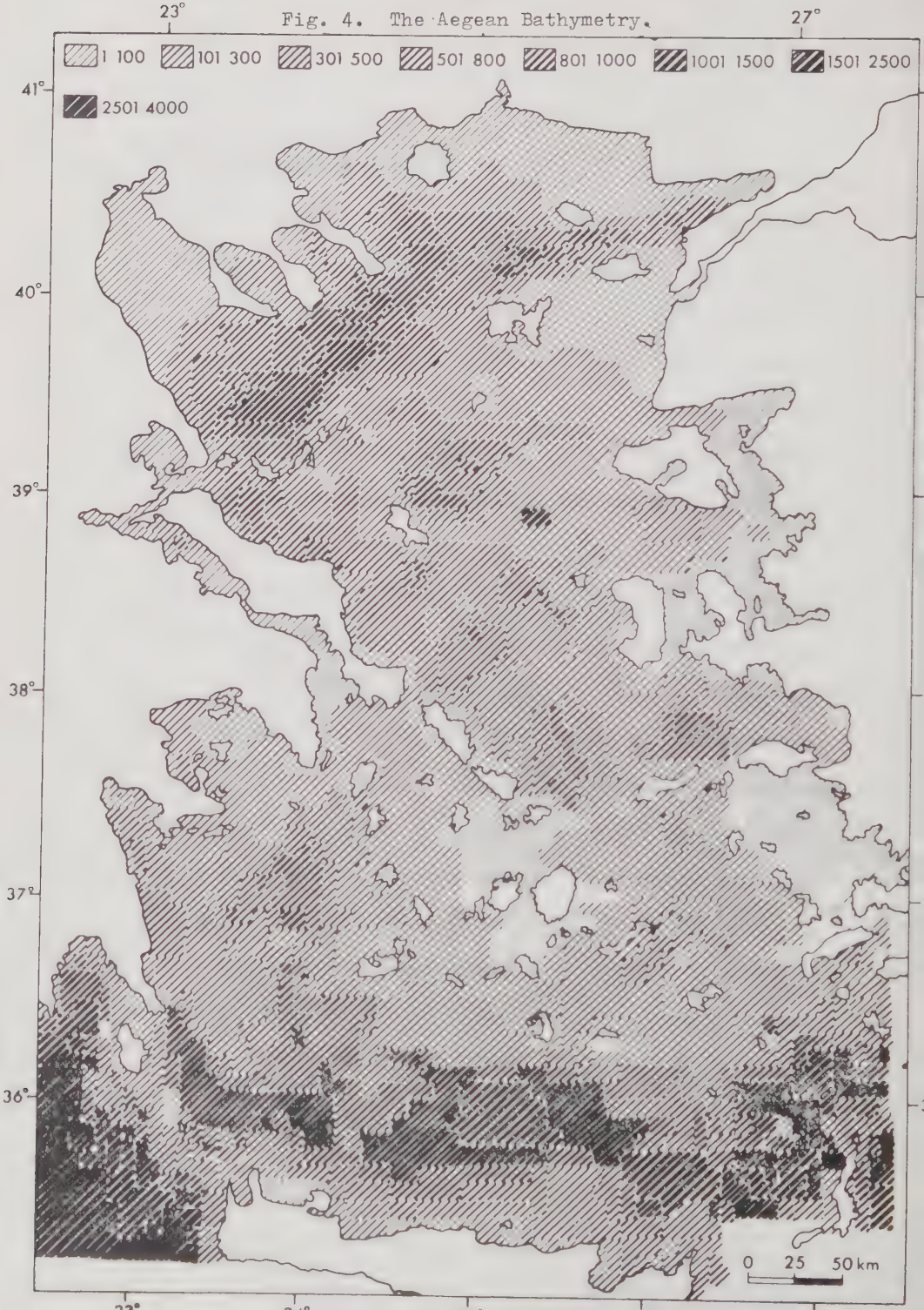

2.3. Existing information.

The existing information concerning the tides of the Aegean basin are rather limited. Sterneck 1914, 1915, gives the first orders of magnitude for tides concerning the NAB and later on Tenani 1930, who studies in more detail the tides of the Dodecanesos islandic complex, (for a summary of both works see Defant 1961). A nodal line of the co-oscillating tide N of the island Leros followed by a list of harmonic constants for some islands of the eastern Aegean, were computed by Tenani 1940. A spectral analysis of recent tidal records from two sites of the Aegean (Kavala at NAB and Heraklion, Crete) -see Chapter 3, paragraphs 3.3; 3.4; 3.5- as well as the older constants, confirm the modest tides of the Aegean which do not exceed the 10 cm for the semi-diurnal waves.

The most exciting tidal phenomenon within the Aegean is the celebrated current of Euripos, the norrows between the Hellenic mainland's coast and the island of Euboea. Miaoulis -the naval hero of the Greek War of Independence- and Forel 1879 were the first who studied the phenomenon in the recent centuries. Kruemmel 1888, Endrös 1914, Sterneck 1916

studied as well the problem from the hydrodynamical point of view (summarized by Defant 1961), while Veis 1954 constructed Tables on the current's movements still in use today,(see for instance Variaghin 1972).

The agency in charge for the recordings of the sea tides in Greece is the Hydrographic Service of the Hellenic Navy. The basic aim of the observations is navigation. In Aegean sea are operating about 15 tidal-meters (tidal rods) and four tidal-gauges of floating type (Fig.8); all of them are located inside ports.(For details on these stations see Variaghin 1972). In Fig.5 and Fig.6 are summarized respectively the maximum and the average amplitudes of the recorded tides in cm independently from the levelling reference points to which the sea-tidal instruments are always connected. In Fig.7 the establishment of ports are shown (after Tenani 1940),in hours.

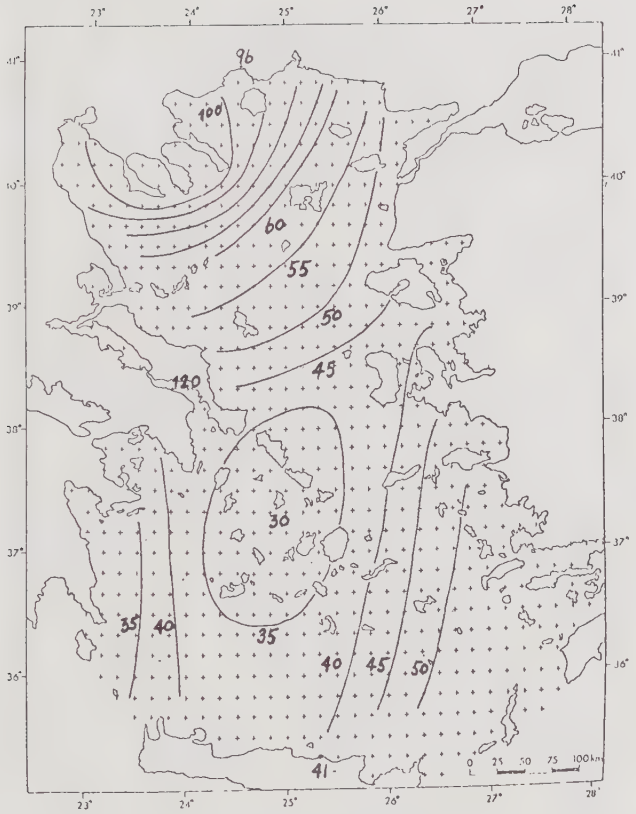

Fig. 5. Propagation of the maximum observed tidal amplitudes in cm.

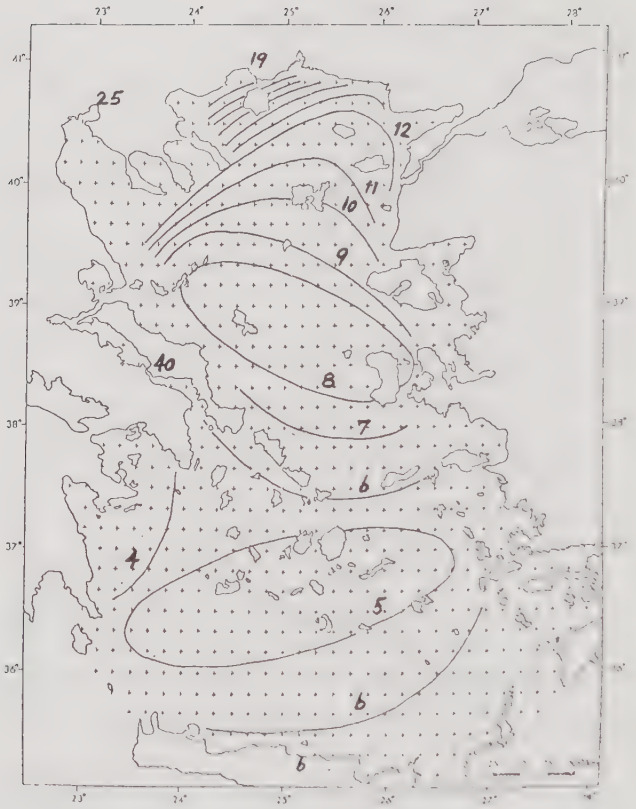

Fig. 6. Propagation of the average observed tidal amplitudes in cm.

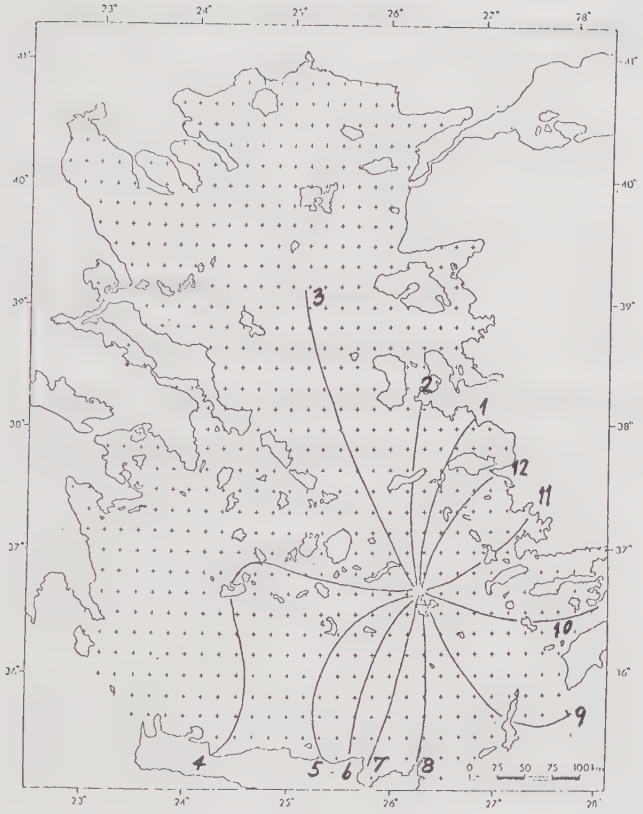

Fig. 7. Establishment of ports in hours.
(after Tenani, 1940).

3. ANALYSIS OF DATA

The analysis of tidal records, being in fact deterministic and not stochastic time series, assuming low noise level, (for a detailed discussion see for instance Bozzi Zadro 1970), could be carried out by several series analysis techniques e.g. harmonic analysis, spectral analysis and least squares analysis, (Shureman 1958, Cartwright and Catton 1963, Murray 1964, Bozzi Zadro and Poretti 1972).

3.1. The general equation

The general equation for the tide-height h at an epoch t could be approximated by:

$$h = h_o + \sum_i A_i \cos(a_i t + \alpha_i) \qquad (3.1.1)$$

where h_o is the mean water level, referred to a used datum, defined either a-priori or a-posteriori.

In the above equations:

The cos(.) terms are called the tidal components.

The coefficients A_i are called the amplitudes of the tidal

components and could calculated by tidal data at each place. The $(a_i t + \alpha_i)$ are angles varying in an uniform way and their values at any epoch t are the phases.

The coefficients a_i of the epoch t represent the variation rate of the phase and is called the velocity of the tidal coefficients (units: degrees per hour).

The time required, for the tidal component, to pass a whole cycle is called period and is computed by dividing 360° by the velocity of the components.

The periods and the corresponding tidal components' velocities are computed by means of astronomic quantities being independent of the location of the place.

The α_i are referred to the starting phases of the tidal components' angles for t=0. The starting phases are dependent on the location and on the instant the time starts counting. Their values are computed by the tidal observations.

3.2. The method of analysis.

As we have said before there are three distinct types of tidal analysis, discussed in details in the time series

Fig. 8. Aegean sea. Sites with tidal stations.

analysis litterature. In this study the tidal constants that have been used in order to constrain the numerical solution of the hydrodynamic equations for the Aegean sea, were those given by Tenani 1940, carried out by the classical harmonic methods and the recent ones for the ports of Kavala and Heraklion, given in Chapter 3, prgrph. 3.3, performed by the use of spectral analysis techniques.

The two sea tidal stations Kavala (KAV) and Heraklion (HER) are located at the North NAB (φ = 40°.9325 N, λ =24°.4147 E) and the South SAB (φ=35°.3433 N, λ =25°.1400 E) respectively. The recorded maximum and mean amplitudes of these ports are shown at Fig.5 and Fig.6. At both places are operating floating-type tide-gauges the one of KAV being more recent with higher resolution, recording in a 1/10 scale and providing weekly records, while the one at HER records in a 1/5 scale and provides 2-weeks records. The location of the tide gauges within the two ports are shown in Fig.9 (for more information see Variaghin 1972).
The records available for the analysis were selected in order to satisfy the requirements for the more recent and best quality data, concerning as well the continuity of the curves for the shake of the digitalization.

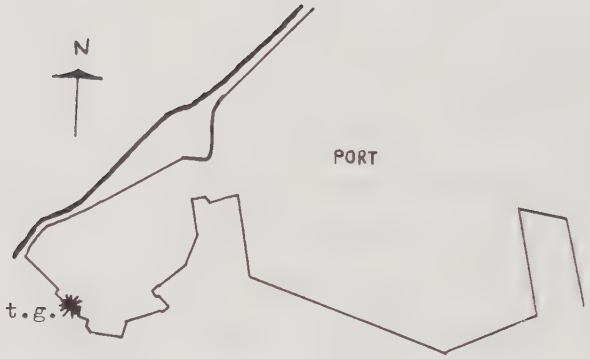

HER, scale 1/7500

KAV, scale 1/10000

Fig. 9. Location of the tide-gauges within the ports of Kavala and Heraklion.

The suitable records for KAV covered the period of 10 months (January to October 1975) while the records of HER the period of only 3 months (August to October 1975).
The records have been digitalized by means of a cartographic digitalization machine (Calma type), at the Osservatorio Geofisico Sperimentale (OGS) of Trieste, Italy, associated with a magnetic tape-storage recorder. The resolution base of the machine's x-y grid, selected for the digitalization, was 0.01 inches which corresponds to 0.25 mm and translated to time interval -concerning the records- corresponds to about 10 min. Due to the high resolution of the digitalization and the accuracy limitations of the records, concerning the time requirements, we digitalized the KAV records independently for each month. The records of HER were unified in one serie. The programme for the intepretation of the Calma's magnetic tape storage to the language of a CDC 6400 computer of the University of Trieste, was provided by Dr. B.B. Manca of the OGS.

3.3. Analysis for KAV and HER.

The method of analysis preferred was the spectral one for the following reasons:

i. The spectral method of analysis provides a global overview of the phenomenon, detecting energies on frequencies which differ from the theoretical ones, especially concerning sea tidal data, as well as information on interaction phenomena between tide components, e.g. shallow water tides and at seiches frequencies.

ii. We can apply always suitable ideal filters (see for instance Godin 1971) before the transformation which could always delete contamination effects, while in harmonic analysis the filters are in general constructed under the bias of a unit transfer function at an a-priori defined frequencies, without taking into account other eventually important tidal frequencies.

iii. The errors appearing in the spectral analysis method can be easily determined or reduced to negligible quantities.(For a detailed discussion see Bozzi Zadro and Poretti 1971, 1972).

The time series have been modulated by the usual D2 Hamming window (see for instance Blackman and Tukey 1958), and runned into a CDC 6400 computer of the University of Trieste through the subroutine FOURT based on the Cooley and Takey

algorythm for the computation of the Fast Fourier Transform (Cooley and Takey 1965). The width of the elementary frequency band which has been solved is of the order of 1.4×10^{-3} cph for KAV and of about 4.6×10^{-4} cph for HER (corresponding to one and three months analysis respectively). Taking into account that for the diurnal tidal components K1, S1, P1, M1, O1 the frequency differences between each component and the successive one is varying between 1.1×10^{-4} and 1.5×10^{-3} cph and for the semidiurnal waves K2, S2, M2, N2 between 2.3×10^{-4} and 2.8×10^{-3} cph, it was not possible to avoid overlappings of the djacent spectral energies. The phases are highly affected by errors when contamination of adjacent spectral energies occurs, as well as when the actual frequencies of the time series are slightly different compared with the derived frequencies. For this reason was necessary the improvement of the phase results applying an interpolation method described by Bozzi Zadro and Poretti 1972. All spectral values have been shifted in phase in order to obtain a common starting time -the starting time of the first time serie-. The phase modulation due to the angle u (see Shureman 1958), depending on the lunar nodes, has been taken into account as well.

3.4. The results

In Fig.10 and Fig.11 the logarithms of spectral amplitudes for KAV and HER are given as frequency functions in hourly periods. In Tab.1 and Tab.2 the values of spectral amplitudes are summarized for diurnal and semidiurnal waves as well as for some remarkable terdiurnal ones, detected from the KAV registrations; the underlined peaks of the spectral amplitudes concern the corresponding solved periods. In Tab.3 the KAV results are given for the diurnal and the semidiurnal waves P1, S1, K1 and M2, S2, K2 respectively, for the first month and for its combinations with the successive months; the phases are referred to the starting time 6^h GMT, 1 Jan. 1975. At the last row of Tab.3 the g epochs of the corresponding waves are computed, from the tenth row phases and from the astronomic Greenwich arguments V_o+u described in detail by Shureman 1958, who gives as well Tables concerning the values V_o+u, for the beginning of each calendar year, from 1850 up to 2000, (see p. 75-78 and p. 210, 212,217).

From the obtained results we could discuss the following:

i. Concerning the KAV registrations, though the high noise

level (about 0.1 cm), and the low signal to noise ratio, mainly because of the quality of the records, the main groups of the neighbouring frequency waves as well as lower tidal amplitudes were easily recognized. In Tab.1 the well distinguished diurnal group P1, S1, K1 is given having a mean amplitude of about 3 cm, modulated throughout the year, most probably due to meteorological conditions -max in June and presumably January, min in March and presumably September-. The other waves of the group namely O1 and M1 appear overlapped, but not well distinguished due to both the large width of the elementary frequency band and the narrow width of the amplitudes involved.

For the semidiurnal waves we have the S2 and K2 group with varying amplitudes between 2.7 and 8.5 cm. The M2 is rather well separated with mean amplitude of about 7 cm but we have to consider the N2 -which has low amplitude in general- as contaminating the energy of M2.

Surprisingly a terdiurnal wave was recognized as well, the S3, having an amplitude less than 1 cm. Its origin is judged as meteorological.

As far as the phases are concerned we obtained values highly affected by errors due to the quality of the registration.

Nevertheless we could give a reliable estimation summarized in Tab.3, where the wave-by-wave consistency of the results can be discussed according to the stability achived adding the monthly amplitude and phase values, noticing that the errors in phases are reciprocally proportional to the amplitudes.

Among the diurnal waves, P1 seems to be the most consistance. Among the semidiurnal waves the M2 and S2 appear to be well separated and stable in time. Disregarding the decreasing amplitude values in this Tab. (is always so, when using the interpolation method disturbed by high noise level and uncertainty in timing), the most reliable value for g is estimated to be around 329° for the diurnal waves and varying from 108° to 125° for semidiurnal waves.

The above values are in agreement with the following considerations:

a. It is very well known that neighbouring frequency waves have neighbouring g values at the same place.

b. Diurnal waves have approximately the same phase values in the whole Aegean, as derives later in this work, after the solution of the hydrodynamical equations for the Aegean.

c. The diurnal harmonic constants available for a number

of sites at the Aegean coasts, those of Tenani 1940, are varying from 303° to 355° for the islands of Leros and Kos.

d. The semidiurnal waves in the northern Aegean basin have small phase variations, as it will be shown later in this paper.

e. The phases given by Tenani 1940 for the semidiurnal waves at the northern part of the Aegean are: Thessaloniki 128° and 130° for M2 and S2 respectively.

Besides the spectral peaks of mainly astronomical origin, several small amplitude peaks appeared in the KAV spectra as well, -with periods well confermed in nearly all months of analysis- obviously of meteorological nature and tied to seiche-effects. Disregarding very low frequencies where the resolution power is scarse, the largest period computed varies between 57 to 51 hours, followed by periods around the 33 hours -variations from 35 to 31 hours-. A rather strong peak, sometimes more than 1 cm, appears around the 14 hours, with variations from 14.9 to 13.8 hours. At higher frequencies the noise level does not allow a clear detection of energies.

ii. The HER results are summarized in Tab.2. The elementary

frequency band is about the 1/3 of the elementary frequency band of the previous analysis, so that a better separation of the harmonic constituents can be achived. The signal to noise ratio is worse here, since the tidal energies are too low and the noise too high. The max amplitude of the diurnal waves appears close to the main group P1, S1, K1 and it is 1.5 cm -shifted by one band frequency towards lower frequencies-; O1 has a small amplitude of 0.9 cm. A strong peak characterizes the semidiurnal wave K2 having 2.0 cm amplitude. N2 and M2 are not well resolved since their energies are spread over three neighbouring frequencies. For the phases the same uncertainty appeared, as above, and only the K2 wave has been taken into account, since it is the highest detected and the corresponding computed frequency is very close to the actual astronomic one. The phase computed by means of the spectral analysis is -156°; the astronomic Greenwich value V_o+u for 5^h GMT, 1 Aug. 1975 is 64°; the g epoch results to be 222°.

Unfortunately no other data are available for comparisons concerning this area of the Aegean sea. Other peaks appearing outside the tidal frequency range, have been disregarded due to the high noise level.

		Astr.Perd. (h)	JAN Perd. (h)	JAN Ampl. (cm)	FEB Perd. (h)	FEB Ampl. (cm)	MAR Perd. (h)	MAR Ampl. (cm)	APR Perd. (h)	APR Ampl. (cm)	MAY Perd. (h)	MAY Ampl. (cm)	JUN Perd. (h)	JUN Ampl. (cm)	JUL Perd. (h)	JUL Ampl. (cm)	AUG Perd. (h)	AUG Ampl. (cm)	SEP Perd. (h)	SEP Ampl. (cm)	OCT Perd. (h)	OCT Ampl. (cm)
Diurnal	O1	25.8194	25.66	.9	25.85	1.0	25.72	.6	25.72	1.0	25.66	1.3	25.71	1.1	25.85	1.9	25.71	1.6	25.66	1.6	25.66	1.6
	M1	24.8332	24.80	1.4	24.89	.3	24.83	1.5	24.83	1.7	24.80	1.7	24.83	1.7	24.89	1.7	24.83	1.4	24.81	1.5	24.81	.3
	P1	24.0659																				
	S1	24.0000	24.00	3.3	24.01	2.6	24.01	2.5	24.00	3.1	24.00	3.3	24.00	3.5	24.00	3.1	24.00	2.3	24.01	1.0	24.01	1.3
	K1	23.9344																				
			23.25	1.6	23.18	1.7	23.23	1.3	23.23	1.6	23.25	1.9	23.23	1.6	23.17	1.2	23.23	1.2	23.26	.4	23.26	1.2
Semi-diurnal			12.83	1.3	12.92	2.7	12.86	1.7	12.86	2.7	12.83	1.1	12.86	.7	12.92	1.2	12.86	1.3	12.83	3.2	12.83	1.2
	N2	12.6584	12.61	4.2	12.68	1.9	12.63	3.1	12.63	6.6	12.61	5.8	12.63	6.1	12.68	4.6	12.63	4.8	12.61	7.9	12.61	2.9
	M2	12.4206	12.40	7.2	12.44	6.6	12.42	6.8	12.42	7.2	12.40	7.2	12.41	6.7	12.44	6.6	12.41	8.0	12.40	4.0	12.40	7.8
			12.20	5.3	12.22	7.1	12.21	4.4	12.21	3.4	12.20	2.7	12.20	2.7	12.22	.6	12.20	1.4	12.20	6.0	12.20	5.0
	S2	12.0000	12.00	5.7	12.00	8.5	12.00	6.9	12.00	5.7	12.00	4.6	12.00	2.7	12.00	4.6	12.00	5.0	12.00	3.4	12.00	5.7
	K2	11.9672																				
			11.81	2.7	11.79	4.6	11.81	3.1	11.81	1.4	11.81	1.8	11.80	.7	11.79	1.2	11.80	3.0	11.81	.5	11.81	3.8
Ter-diurnal	S3	8.0000	8.00	.3	8.10	.5	8.00	.4	8.00	.2	7.80	.4	8.18	.7	8.00	.3	7.00	.4	8.10	.3	8.20	.4

Table 1. KAV

DIURNAL			SEMIDIURNAL		
	Astrn. perd. (h)	Comp. perd. (h)	Comp. ampl. (cm)	Astrn. perd. (h)	Comp. perd. (h)	Comp. ampl. (cm)
		26.09	.9		12.80	1.2
O_1	25.8194	25.76	.6		12.72	1.7
		25.43	.4	N_2 12.6584	12.64	1.6
		25.11	.2		12.56	1.8
					12.48	1.5
M_1	24.8332	24.81	.4			
		24.50	.8	M_2 12.4206	12.40	1.5
		24.21	1.5		12.33	.6
P_1	24.0659				12.25	.5
S_1	24.0000				12.18	.6
K_1	23.9344	23.92	1.4		12.10	.8
		23.64	1.2	S_2 12.0000	12.03	1.3
				K_2 11.9672	11.96	2.0

Table 2. HER.

P_1		S_1		K_1		M_2		S_2		K_2		Months of analysis
Ampl. (cm)	phs. (°)	Ampl. (cm)	phs. (°)	Ampl. (cm)	phs. (°)	Ampl (cm)	phs (°)	Ampl (cm)	phs (°)	Ampl (cm)	phs (°)	
128.0	105	229.1	- 59	106.1	145	7.9	-17	8.2	92	4.9	3	I
8.7	-147	19.1	87	9.6	- 51	6.8	- 4	11.6	66	6.1	-56	I+II
4.8	126	1.8	2	.3	156	6.5	-18	8.0	86	2.3	- 2	I+III
3.0	142	2.4	117	1.7	21	6.1	-35	6.5	89	.6	28	I+IV
2.7	139	1.9	132	1.7	36	3.9	-57	5.8	84	.4	-81	I+V
2.7	126	1.0	160	1.2	51	1.6	-74	5.2	78	1.1	-82	I+VI
2.3	120	1.3	-173	1.3	72	1.4	-26	4.9	73	1.2	-59	I+VII
2.3	112	1.2	-153	1.0	81	2.1	-29	4.7	68	.8	-44	I+VIII
2.0	115	1.3	-149	1.1	92	1.5	-14	3.8	66	.7	26	I+IX
2.0	111	1.1	-144	1.0	83	2.0	-27	3.9	72	1.1	28	I+X
Ampl.	g	Ampl.	g	Ampl.	g	Amp.	g	Amp.	g	Ampl.	g	Harmonic constants
2.0	329	1.1	54	1.0	17	2.0	125	3.9	108	1.1	352	

Table 3. KAV.

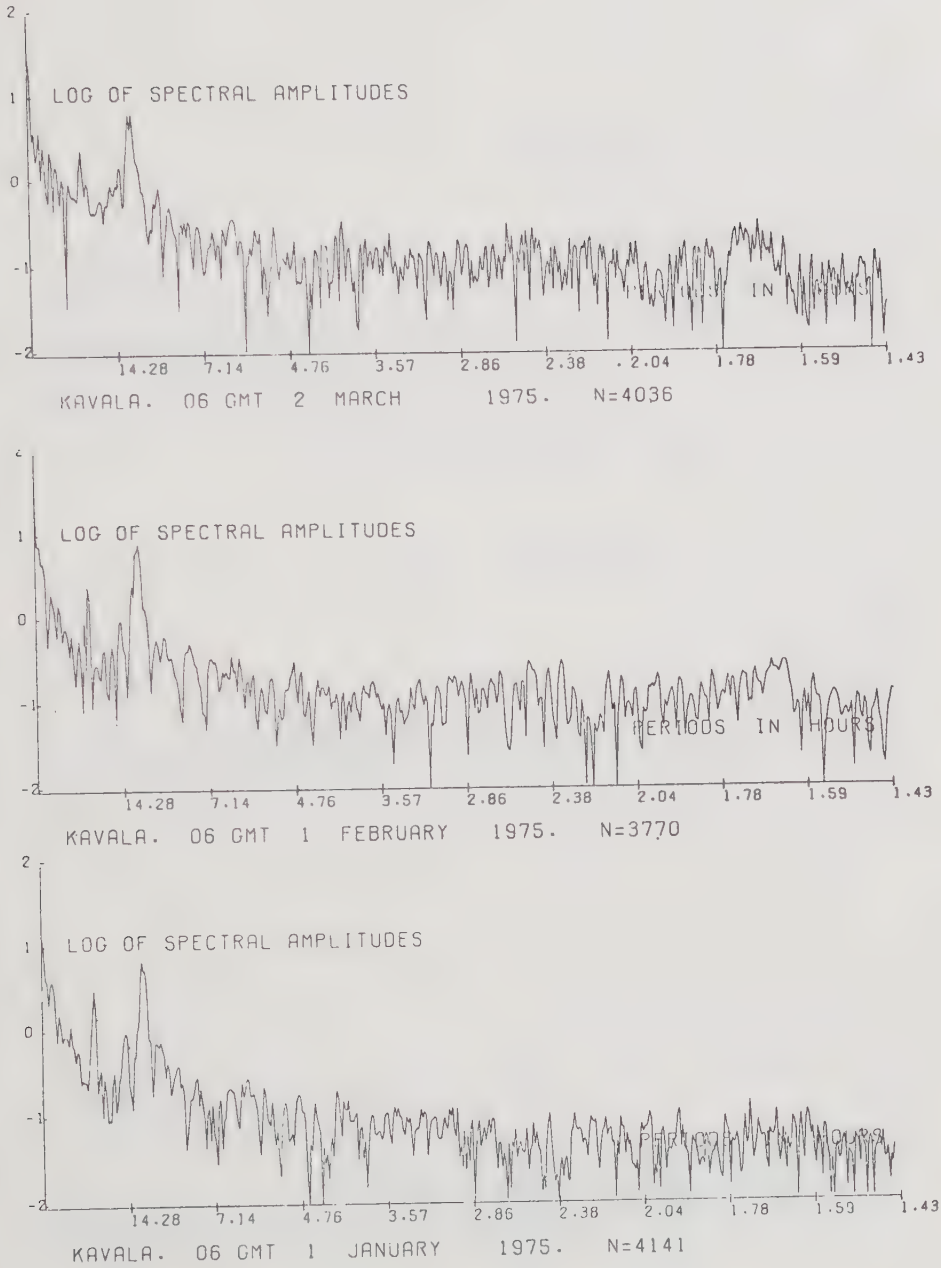

Fig. 10. Logs of spectral amplitudes; Kavala.

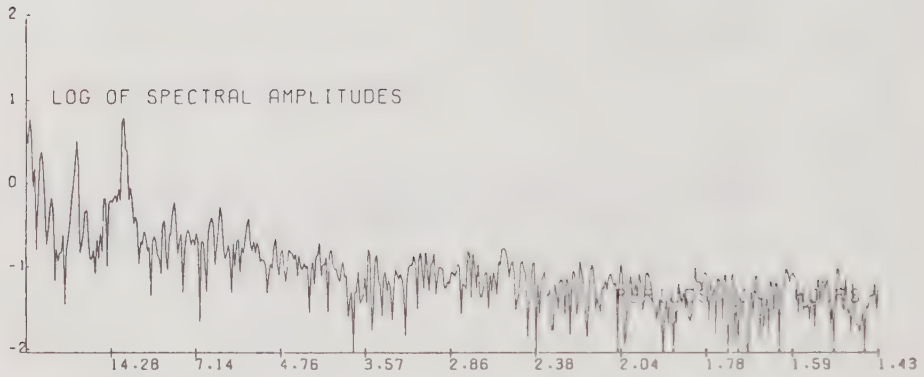

KAVALA. 06 GMT 1 JUNE 1975. N=4035

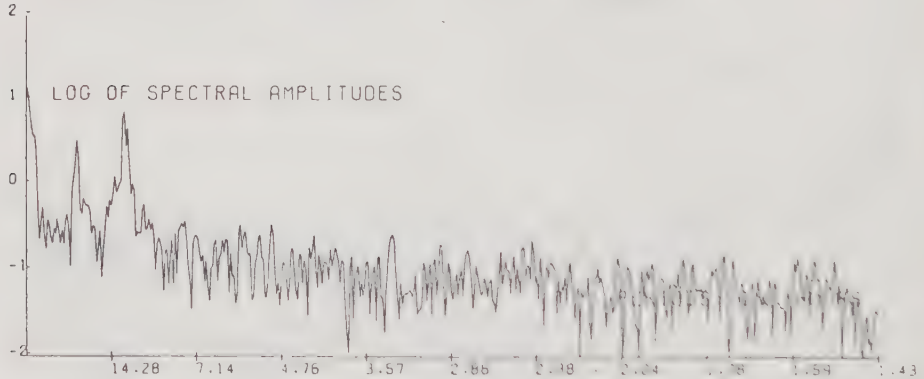

KAVALA. 06 GMT 1 MAY 1975. N=4165

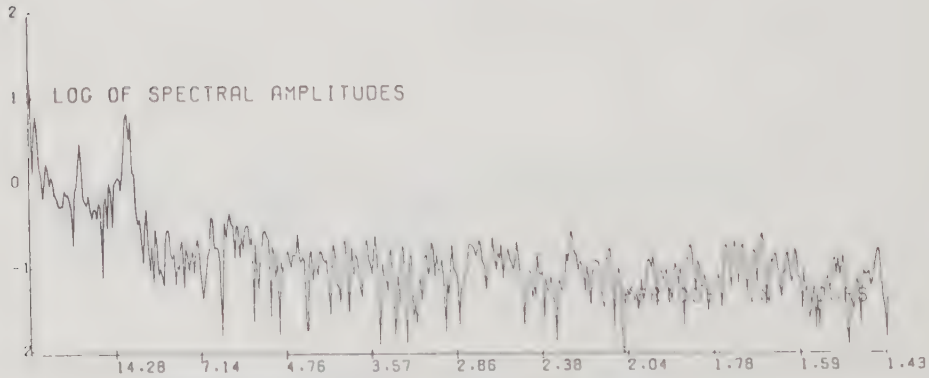

KAVALA. 06 GMT 1 APRIL 1975. N=4044

Fig. 10. (cont.)

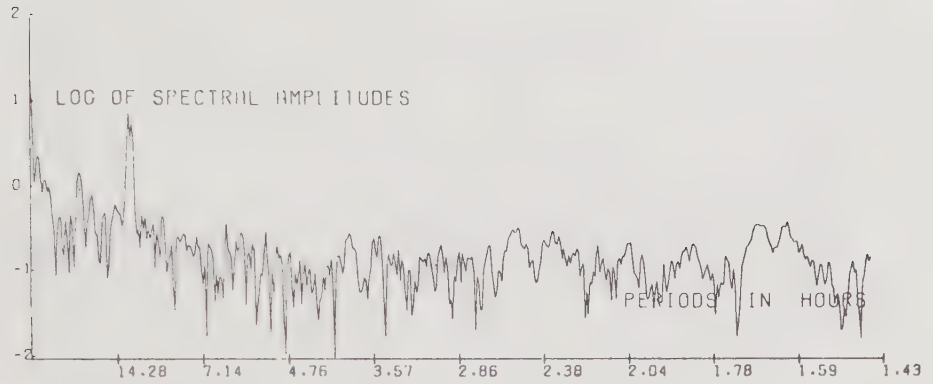
LOG OF SPECTRAL AMPLITUDES
PERIODS IN HOURS
14.28
7.14
4.76
3.57
2.86
2.38
2.04
1.78
1.59
1.43
KAVALA. 06 GMT 1 SEPTEMBER 1975. N=4104

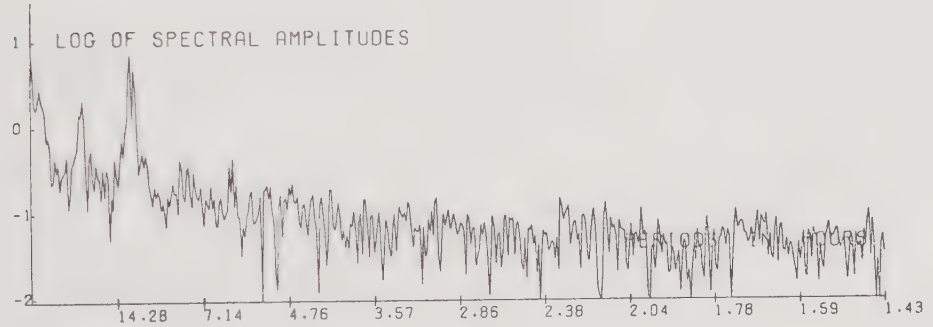
LOG OF SPECTRAL AMPLITUDES
14.28
7.14
4.76
3.57
2.86
2.38
2.04
1.78
1.59
1.43
KAVALA. 06 GMT 2 AUGUST 1975. N=4033

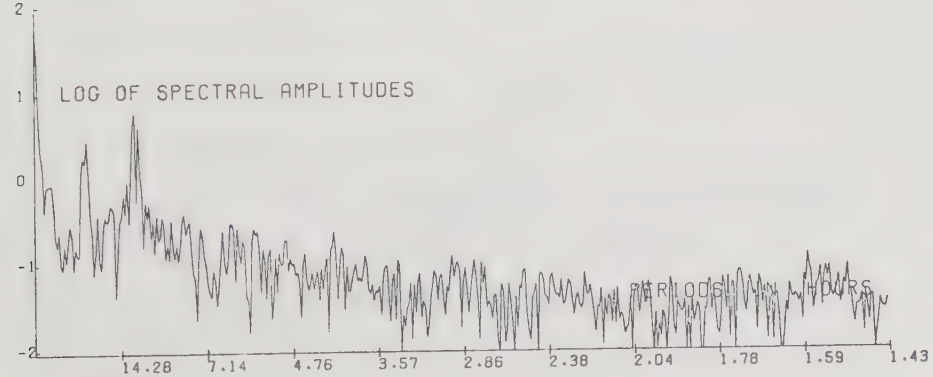
LOG OF SPECTRAL AMPLITUDES
14.28
7.14
4.76
3.57
2.86
2.38
2.04
1.78
1.59
1.43
KAVALA. 06 GMT 3 JULY 1975. N=3755

Fig. 10. (cont.)

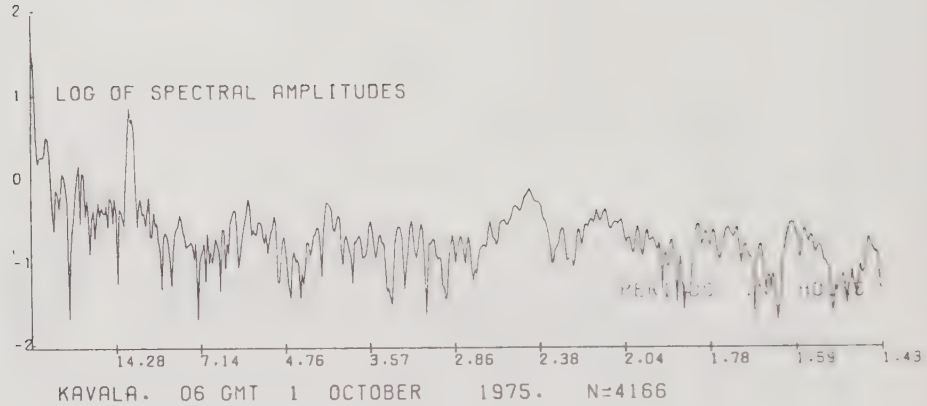

Fig. 10. (cont.)

Fig. 11. Logs of spectral amplitudes: Heraklion.

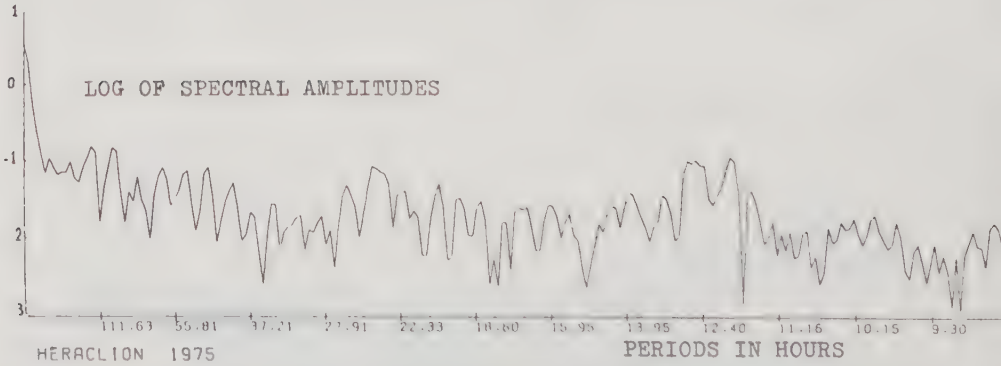

4. SOLUTION OF THE HYDRODYNAMICAL EQUATIONS

The equations in common use in Oceanography for the numerical solution of basin models, are generated by the Navier-Stokes equations (see for instance Hansen 1940 and Defant 1961), constrained by the continuity condition and by the principle of conservation of mass.

4.1. The acceleration of the water particles.

The basic hydrodynamic equations of motion are the "machine" which allows the understanding of the different successive states and behaviour of the water masses.
There are two approaches to attack the problem: The Eulerian approach, due to which we are studying different mass elements when passing from an a-priori fixed point in space; The Lagrangean approach describes, on the other hand, the conditions in the water current towards the course of their displacement. (For more details see Defant 1961).

Lets consider a water element at a point described by its position vector $\underline{x}$ referred to an earth-fixed X, Y, Z

cartesian system (e.g. origin at the geocenter, Z-axis passing from the CIO, as defined by the IPMS; X-axis passing from the mean Greenwich meridian, the Y-axis forming a right handed system.

If $\underline{u}$ is the vector of the velocity components in the direction of the co-ordinates X, Y, Z, we could denote:

$$\underline{x} = \begin{bmatrix} X \\ Y \\ Z \end{bmatrix} \quad , \quad \underline{u} = \begin{bmatrix} u \\ v \\ w \end{bmatrix} \tag{4.1.1}$$

Obviously the eigen-accelerations of the water elements are:

$$\frac{d\underline{u}}{dt} = \frac{d}{dt} \begin{bmatrix} u \\ v \\ w \end{bmatrix} \tag{4.1.2}$$

The eigen-accelerations could be considered in two parts:

i.

$$\frac{\partial \underline{u}}{\partial t} = \frac{\partial}{\partial t} \begin{bmatrix} u \\ v \\ w \end{bmatrix} \tag{4.1.3}$$

which arises from the changes in the state of the motion at $\underline{x}$ and describes a local change.

ii.

$$\frac{\partial(\underline{u}^T)}{\partial(\underline{x}^T)}\,\underline{u} \qquad (4.1.4)$$

which arises from the fact that after an infinitesimal time change dt the water elements are no longer at the initial point $\underline{x}$ but are displaced by the amounts:

$$u\,dt \quad , \quad v\,dt \quad , \quad w\,dt \qquad (4.1.5)$$

which are called the "advective change".

In (4.1.4) we recognize the Jacobian matrix J, being:

$$J = \frac{\partial(u, v, w)}{\partial(X, Y, Z)} = \frac{\partial(\underline{u}^T)}{\partial(\underline{x}^T)} \qquad (4.1.6)$$

Auding now the local and the advective changes we obtain the total eigen-acceleration of each water element under consideration:

$$\frac{d\underline{u}}{dt} = \frac{\partial \underline{u}}{\partial t} + \frac{\partial(\underline{u}^T)}{\partial(\underline{x}^T)}\,\underline{u} = \frac{\partial \underline{u}}{\partial t} + J\,\underline{u} \qquad (4.1.7)$$

Notice here that the partial derivative $\partial/\partial t$ represents the change in the quantity under consideration at a fixed point, while the total derivative d/dt represents the eigen-change in one and the same water-element changing position with time.

4.2. The gradient of pressure.

If ρ is the mass of a unit volume and considering that the only external conservative force is gravity, acting at $\underline{x}$ downwards to the direction of the geocenter, the gradient of the pressure could be written:

$$\text{grad}\ \underline{p} = -\frac{1}{\rho} \begin{bmatrix} \frac{\partial p}{\partial X} \\ \frac{\partial p}{\partial Y} \\ \frac{\partial p}{\partial Z} \end{bmatrix} \qquad (4.2.1)$$

where: $$\underline{p} = \begin{bmatrix} p(X) & p(Y) & p(Z) \end{bmatrix}^T \qquad (4.2.2)$$

4.3. The friction

If the friction is represented by the vectror $\underline{R}$:

$$\underline{R} = \begin{bmatrix} R(X) \\ R(Y) \\ R(Z) \end{bmatrix} = \frac{\mu}{\rho} \begin{bmatrix} \nabla^2 u \\ \nabla^2 v \\ \nabla^2 w \end{bmatrix} = \frac{\mu}{\rho} \nabla^2 \underline{u} \qquad (4.3.1)$$

where $\frac{\mu}{\rho} = \nu$ is called the "kinematic viscocity coefficient", having dimensions ($cm^2 sec^{-1}$) and being already tabulated for μ and ν ; ∇^2 is the well known Laplacian operator.

4.4. The Coriolis force.

If the Coriolis force is represented by the vector $\underline{C}$:

$$\underline{C} = \begin{bmatrix} C(X) \\ C(Y) \\ C(Z) \end{bmatrix} = \begin{bmatrix} 2\omega v \sin\varphi - 2\omega w \cos\varphi \\ -2\omega u \sin\varphi \\ -2\omega u \cos\varphi \end{bmatrix} \qquad (4.4.1)$$

or:

$$\underline{C} = -2\omega \cos\varphi \begin{bmatrix} w - v\ tg\varphi \\ u\ tg\varphi \\ u \end{bmatrix} \qquad (4.4.2)$$

The above expressions are considered sufficient for incompressive fluids, (approximated by the sea-water), as follows from the general theory of friction in liquids. Summarizing all the above developments we could write the basic hydrodynamic equation of motion in the following compact vector-form relation:

$$\frac{d\underline{u}}{dt} = \frac{\partial \underline{u}}{\partial t} + J\,\underline{u} = \underline{C} + \text{grad}\ \underline{p} + \underline{R} \qquad (4.4.3)$$

As far as the Coriolis force is concerned we should notice the following:

The vertical component of the water moving masses could be climinated since acting in the same direction as gravity does, is vanishingly small compared to the latter. Furthermore and under quasi static conditions the difference between gravity and the vertical pressure gradient could be considered of the same order of magnitude as the vertical component of

the Coriolis force, which can be regarded as an increase or decrease of gravity, (Defant 1961).

The equation (4.4.1) is also written as:

$$\underline{C} = -2\,\omega\cos\varphi \begin{bmatrix} w - v\ tg\,\varphi \\ u\ tg\varphi \\ u \end{bmatrix} + \begin{bmatrix} 0 \\ 0 \\ g \end{bmatrix} \qquad (4.4.4)$$

Introducing now (4.1.2),(4.1.3),(4.1.4),(4.2.1),(4.3.1) and (4.4.4) into (4.4.3), we obtain the explicit form:

$$\frac{d}{dt}\begin{bmatrix} u \\ v \\ w \end{bmatrix} = \frac{\partial}{\partial t}\begin{bmatrix} u \\ v \\ w \end{bmatrix} + \begin{bmatrix} \frac{\partial u}{\partial X} & \frac{\partial u}{\partial Y} & \frac{\partial u}{\partial Z} \\ \frac{\partial v}{\partial X} & \frac{\partial v}{\partial Y} & \frac{\partial v}{\partial Z} \\ \frac{\partial w}{\partial X} & \frac{\partial w}{\partial Y} & \frac{\partial w}{\partial Z} \end{bmatrix} \begin{bmatrix} u \\ v \\ w \end{bmatrix} =$$

$$= -2\omega\cos\varphi \begin{bmatrix} w - v\ tg\varphi \\ u\ tg\varphi \\ u \end{bmatrix} + \begin{bmatrix} 0 \\ 0 \\ g \end{bmatrix} - \frac{1}{\rho}\begin{bmatrix} \frac{\partial p}{\partial X} \\ \frac{\partial p}{\partial Y} \\ \frac{\partial p}{\partial Z} \end{bmatrix} + \frac{\mu}{\rho}\nabla^2 \begin{bmatrix} u \\ v \\ w \end{bmatrix} \qquad (4.4.5)$$

Accepting that the oceanic water movements are much larger in the horizontal sense and recalling that w is vanishingly small, (4.4.5) could be as well written, considering $\underline{C} = 0$:

$$\frac{d}{dt}\begin{bmatrix} u \\ v \\ 0 \end{bmatrix} = \begin{bmatrix} 0 \\ 0 \\ g \end{bmatrix} - \frac{1}{\rho}\begin{bmatrix} \frac{\partial p}{\partial X} \\ \frac{\partial p}{\partial Y} \\ \frac{\partial p}{\partial Z} \end{bmatrix} + \frac{\mu}{\rho}\nabla^2 \begin{bmatrix} u \\ v \\ 0 \end{bmatrix} \qquad (4.4.6)$$

4.5. The continuity condition.

The above equations of motion should be conditioned by the continuity equations based on the principle of the conservation of mass.

Assuming an elementary volume, experiments have shown that for the conservation of mass the continuity condition is written by the well known relation:

$$\text{div } \underline{u} = -\frac{1}{\rho}\frac{d\rho}{dt} \qquad (4.5.1)$$

and assuming incompressible liquid, (as we are doing in the numerical solution of the hydrodynamic equations, concerning the sea water) :

$$\frac{d\rho}{dt} = 0 \qquad (4.5.2)$$

thus: $$\text{div } \underline{u} = 0 \qquad (4.5.3)$$

which is the continuity condition for the water.

4.6. Application to natural basins

The formulation of the equations derived above could be significently simplified in the case of basins with modest dimensions and with small water level variations with respect to the depth (as for instance the case of the Aegean sea). These simplifications are summarized in the following assumptions: Homogeneous, incompressive and hydrostatic fluid, concerning the internal pressure field; constant gravity; constant Coriolis force thus negligible radial component; a mean latitude.
The equations could also be linearized eliminating the friction effect, though in some cases it is advisable to include this effect in the linearization using a suitable coefficient of the friction force.(Hansen 1943).

For an harmonic component of frequency σ (Hendershott and Munk 1970), we could write the following system of first order differential equations, called the LTE, (compare with (4.4.5)), concerning the functions u, v and η which replaces here w.

$$\frac{\partial}{\partial t}\begin{bmatrix} u \\ v \\ \eta \end{bmatrix} + 2\,\omega\cos\varphi \begin{bmatrix} -v\ \mathrm{tg}\,\varphi \\ u\ \mathrm{tg}\,\varphi \\ 0 \end{bmatrix} = -\frac{g\,\sec\varphi}{a}\begin{bmatrix} \frac{\partial(\eta-\bar{\eta})}{\partial\theta} \\ \cos\frac{\partial(\eta-\bar{\eta})}{\partial\varphi} \\ \frac{1}{g}\left(\frac{\partial(uh)}{\partial\theta}+\frac{\partial(vh\cos\varphi)}{\partial\varphi}\right) \end{bmatrix} \qquad (4.6.1)$$

where as in paragraph 4.4 θ , φ the longitude and latitude, u, v the velocity components towards the longitude and latitude respectively, η the water level variation with respect to the equilibrium tide $\bar{\eta} = \frac{U}{g}$, U the tidal potential (sum of the Moon and Sun tidal potentials, see Godin 1971 for an elegant derivation), g the gravity, ω the rotation of the Earth, a the mean radius of the Earth and h the basin's depth.

For the numerical treatment of small dimension basins, where the influance of the curvature of the Earth could be ignored it is more convenient to adopt cartesian coordinates, as in paragraphs 4. If the basin under consideration communicates directly with the open sea, the astronomic tide could be neglected since the movements of the water masses within the basin are almost completely dependent on the imposed oscillations from the open sea thus on the input conditions at the entrance connecting the open sea with the basin.

Wishing to study only the variations of the basin's water level using simple derivations and substitutions in the formulation of the equations, we conclude to the following differential equations of the elliptic type, concerning now only η (Hansen 1943). Designing these well known elliptic second order partial differential equation we have to assume that the water elevation and the cartesian components of the velocity are proportional to $\exp(i\sigma t)$, where σ the frequency and t the time.

$$\nabla^2\eta + \frac{\partial\eta}{\partial X}\left(\frac{\partial lgh}{\partial X} + \frac{f}{\lambda}\frac{\partial lgh}{\partial Y}\right) + \frac{\partial\eta}{\partial Y}\left(\frac{\partial lgh}{\partial Y} + \frac{f}{\lambda}\frac{\partial lgh}{\partial X}\right) - \frac{i\sigma(\lambda^2+f^2)}{hg\lambda}\eta = 0 \qquad (4.6.2)$$

where $\lambda = i\sigma + \beta$

β being the linear friction coefficient.

The equation (4.6.2) could be derived by approaching the problem in the following ways:

i. As a Dirichlet problem, when the values are given at the boundary of the domain, searching to determine the solution within the boundaries. For closed basins it is necessary to know the solution along the coastal lines; for partially open basins communicating with the open sea

through openings, it is necessary to assign the values either along the coastal lines or along a line which bounds the basin from the open sea.

ii. As a Neumann type problem, assigning the derivatives of the unknown function η along the boundary. Assuming that the water flows parallel to the coastal lines, we could derive linear relations between the derivatives of the unknown function along the coast, which follow the equations of motion.

Similar relations could be assigned at the opening line which bounds the basin from the open sea and could be therefore derived just knowing the velocity; in such a case the solution is determined apart a constant.

iii. As a mixted problem, using Neumann-type conditions assigned along the coast and the Dirichlet conditions at the opening. This last way is considered as the most realistic one when we are treating natural basins.

In the present work we are using this last solution applying the Neumann-type at the points along the coastal lines and the Dirichlet-type conditions at the opening line as well as at central points where the solution was a-priori known.

The Neumann-type conditions used here, for points along the coast are, (Baxa et al. 1971):

$$\begin{bmatrix} f & -\lambda \\ \lambda & -f \end{bmatrix} \begin{bmatrix} \frac{\partial \eta}{\partial X} \\ \frac{\partial \eta}{\partial Y} \end{bmatrix} = \begin{bmatrix} 0 \\ 0 \end{bmatrix} \qquad (4.6.4)$$

the first row condition concerning the coastal line parallel to the X-axis, while the second row condition for the coastal line parallel to the Y-axis.

4.7. The formation of the grid.

For the numerical solution of the hydrodynamical equations the basins are usualy covered by a preselected grid of parallel and perpendicular lines -e.g. Mercator squares- the nodal points being their intersections.
At all nodal points either along the coast or within the main basin, should be associated a finite difference equation derived from the discretization equation (4.6.2).
In the present work the computational layout of the above mentioned derivatives is the following:

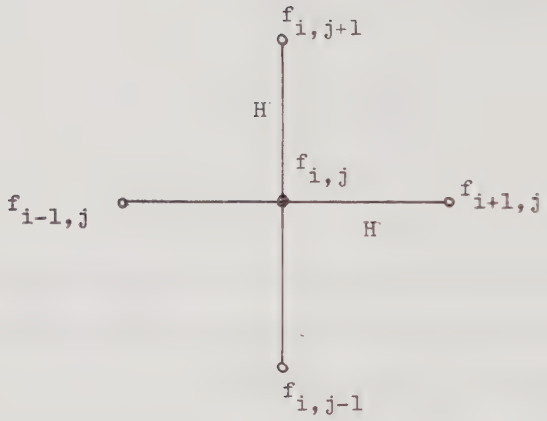

Fig. 12. 5-points cross type descretization design.

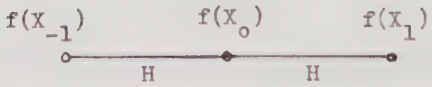

Fig. 13. 2-central points descretization design.

i. For the calculation of the ∇^2 we used the 5-points cross type design:

As an example of the discretization procedure of second order partial differential equation we are using the Poisson equations:

$$\nabla^2 f(X,Y) = g(X,Y) \tag{4.7.1}$$

where f is given on a closed boundary which in our case is rectangular. We discretize the continuous functions $f(X,Y)$ and $g(X,Y)$ by functions at the nodal points of the grid. If:

$$f_{ij} = f(X_i, Y_j) \tag{4.7.2}$$

where X_i, Y_j is a nodal point, then similarly:

$$g_{ij} = g(X_i, Y_j) \tag{4.7.3}$$

In order to express the partial derivatives, we could write (4.7.1) in the Lagrangean form:

$$\begin{bmatrix} & f_{i,j+1} & \\ f_{i-1,j} & -4f_{i,j} & +f_{i+1,j} \\ & f_{i,j-1} & \end{bmatrix} = H^2 g_{ij} \qquad (4.7.4)$$

where the terms are positioned in correspondance with the nodal points of the grid and H is the discretization step. Furthermore (4.7.4) could be re-written in a matrix form:

$$\begin{bmatrix} 0 & 1 & 0 \\ 1 & -4 & 1 \\ 0 & 1 & 0 \end{bmatrix} f_{ij} = H^2 g_{ij} \qquad (4.7.5)$$

where the 3x3 matrix represents an operator or template which can be attached anywhere on the grid. The resulting discretization error is of the order of H^2. The above matrix-operator can be associated to points adjacent to the boundary and obviously values of f corresponding to points on the boundary will appear within the equations as constants and not as unknowns. From the above design we could construct easily the design matrix of the system of the hydrodynamic equations, which is not of course symmetric. Points that are adjacent on the grid are close together in

the matrix if they are lying in the same row otherwise there are wide apart. Fictitious points outside the integration domain could be used when we are dealing with boundary conditions involving derivatives as we are doing in our cases. In the next paragraphs the matrix-discussion will enter into dimension, symmetry and computation problems.

ii. For the computation of the first derivatives, the simplest way should be the use of the 2 adjacent design (backward or forward differentiation):

$$\frac{df}{dX} = \frac{f(X_1) - f(X_o)}{X_1 - X_o} \qquad (4.7.6)$$

or:

$$\frac{df}{dX} = \frac{f(X_o) - f(X_{-1})}{X_1 - X_o} \qquad (4.7.7)$$

the discretization error being in this case of the order of $H=X_1-X_o$. An error of the order of H^2 is obtained when central differences design is used, as in the present work:

$$\frac{df}{dX} = \frac{f(X_1) - f(X_{-1})}{X_1 - X_{-1}} \qquad (4.7.8)$$

4.8. On the matrix analysis of the system.

As we have said before, we need to use some fictitious points, namely earth points adjacent to coastal points, in order to associate the first and the second derivatives conditions at the coastal points. The unknowns corresponding to the fictitious points should be a-priori eliminated, combining in a suitable way the two equations concerning the coastal points.

Following the design analyzed above, at any point where the solution in unknown, corresponds a linear equation which relates the values of the unknown function η referred to the adjacent points at the same point. The matrix of the coefficients of the system, (called from now on the design matrix), results to be a complex square matrix with a minimum of 5 non-zero elements per row. The dimension of the design matrix A is equal to the number of the nodes involved in our basin model, thus equal to the unknowns.
When we have known tidal values at the basin's boundaries -coastal or not-, the corresponding equation of the system could be eliminated replaced by the nodal value.

The linear system to be solved is formulated in matrix notation as:

$$A \underline{x} = \underline{l} \qquad (4.8.1)$$

where $\underline{l}$ the vector of the known terms and $\underline{x}$ stands for the vector of the unknowns being identical to the vector $\underline{\eta}$. $\underline{l}$ is vanishing in adiabatic conditions, if we eliminate the influence of the external forces. In this case the system turns to be homogeneous,(see any Matrix Calculus text book). The vector $\underline{l}$ is not completely zero having some non-zero elements when the solution is known at the corresponding grid points.

Because of the rather high number of the unknowns -or of the design matrix- involved in a numerical solution of the hydrodynamic equations even for basins with modest dimensions,(e.g. the Aegean sea), it is necessary to use special programming techniques for the computer solution, utilizing all the advantages of the band design matrix.
It is well known that differential equations provide always banded systems thus band design-matrices, as happens in

our cases. Using special matrix storage techniques in a reasonable computer of, say, 250 microsecond multiplication time and of about 16000 words of core storage, we can process band matrix equations in large sets, of some thousands, with the solution time incresing linearly with the dimension n of the design matrix, while for general systems without band structure of the design matrix, the time reaches the third or the fourth power of the dimension.

There are several ways for solving linear systems: direct methods, indirect methods like the triangular form, the pivot-condensation, the iterative methods or the relaxation method, (see for instance any Numerical Analysis text book). The direct methods, -elimination process-, should be preferred in general, but when the number of the equations they have to be solved is relatively high the indirect methods are considered more realistic, like the Gauss-Seidel method which depends strongly on whether the design matrix of the system converges in the iteration process. In our cases, for the solution of the hydrodynamic equations, when the design matrix arises from differential equations thus is a band matrix, we have a "strong diagonal" compared with the off-

diagonal elements and convergence always there, as it is shown in practice.

From the above discussion it is well understood that for large basins it is not possible to obtain the full inverse matrix output of the design matrix, limiting ourselves on the solution only. Nevertheless, in many cases it is possible, using a special modeling of the basin, for instance larger grid and of course a rather large computer, to invert the design matrix and to obtain in this way valuable information cencerning the transfer functions of the basin as we will see later on. Another important thing we could achive with the low-dimension models is the computation of the eigenvalue spectrum of the design matrix, which is in general a rather time consuming computer process. The eigenvalues of the design matrix are directly connected with the eigenfrequencies of the basins.

It should be stressed here the influence of the rounding-off errors in the numerical computer process which reflects on the singularity behaviour of the design matrix. Many times appears a numerical singularity without the existance of the algebraic singularity and vice-versa. There are

techniques which allow the detection of the singularity status of the design matrix without the danger of using only the determinant as a singularity criterion. (For an elegant discussion see La Porte et Vignes 1974 as well as Wilkinson 1960,1963 for general topics.).

4.9. Impulse response, eigenfrequencies.

Turning now back to our main subject which is the solution of the hydrodynamic equations of basins, lets try to combine the ideas developed above.

By eliminating the external forces and in adiabatic conditions, (zero level values at the opening, vanishing of the normal component of the velocity along the coast), the system (4.8.1) is reduced in an homogeneous one. If m values are assigned at the basin's entrance, the vector $\underline{1}$ has m non-zero elements which correspond to the equations associated to the m assigned values at the entrance. Due to the linear nature of the system, it follows that the response at any internal point could be considered as a sum of m-responses derived from the adiabatic conditions at the boundary, with the input data assigned successively only at

one of the m entrance points:

$$x_i = \bar{a}_{ik}\, l_k \qquad (4.9.1)$$

where $\bar{a}_{ik}$ the corresponding ik element of the inverse A^{-1} of the design matrix, with the summation convention running over k. In the same way the $\bar{a}_{ik}$ element of the A^{-1} matrix associated with a basin in adiabatic conditions, represents the response at a point P_i within the basin, caused by a pulse at a point P_k. The level variation at a point P_i caused by a unit variation of the level at the point P_k will be given by means of the amplitude and phase, from the relation:

$$F_{ik} = \frac{\bar{a}_{ik}}{\bar{a}_{kk}} \qquad (4.9.2)$$

where the function F_{ik} represents the transfer function value at the given frequency σ, between the input at P_k and the output at P_i.

For the study of the behaviour of the basin influenced by atmospheric effects, having a predictable origin, it is advisable to materilize the phenomenon computing the transfer

function as frquency function along selected profiles of the basin. The analysis of the basin's responses as frequency function would be simplified by the two dimensional representation of the transfer function in relation to the frequencies and the distances along the assigned profile. Having already analyzed the importance of the inverted design matrix, lets see the interesting information that the the eigenvalue spectrum of the design matrix could give us.

Christensen and Groves 1970, Christensen 1972 and Platzman 1972,1975, have shown the way for the determination, in some cases, of the eigenfrequencies of the basins examining for what values of the impressed frequency, the matrix A is algebraically singular.

From the discretization of (4.6.2) multiplied by gh and in absence of friction, it follows:

i. If the basin has constant depth, the imposed frequency affects always only the diagonal elements a_{ii} of the matrix A :

$$a_{ii} = -2 \left(\frac{1}{\Delta X^2} + \frac{1}{\Delta Y^2} \right) gh - (f^2 - \sigma^2) \qquad (4.9.3)$$

where ΔX, ΔY are the discretization steps towards the X,Y axes.

ii. If the basin has a variable depth and the Coriolis force is vanishing, the imposed frequency σ affects always only the diagonal elements a_{ii} of the design matrix A :

$$a_{ii} = -2 \left(\frac{1}{\Delta X^2} + \frac{1}{\Delta Y^2} \right) gh + \sigma^2 \qquad (4.9.4)$$

Analyzing the matrix A by algorythms in use for the numerical process of real matrices, we could split each equation of the system in two equations corresponding to the real and to the imaginary term of the original equation. The matrix B obtained by this way has obviously dimensions 2nx2n. Rearranging in a proper way the rows and the columns of the B matrix, its diagonal elements b_{ii} have the same characteristics with the a_{ii} elements. It is well understood that in the case of a basin with constant depth it is sufficient to examine the real part, -real submatrix of nxn dimensions-, of the enlarged design matrix B, considering the numerical equality of the real and the imaginary submatrices within the B. Observing (4.9.3) and (4.9.4) it follows clearly that the eigenvalues $eig(.)_i$ of the matrix B are related with the eigenfrequencies S of the basin, by the equation:

$$S_i = \pm \left(\sigma^2 - \mathrm{eig}(B)_i \right)^{1/2} \qquad (4.9.5)$$

The above eigenfrequencies correspond to the high frequency gravitational modes of the basin. In more general cases, when the basin follows the rotation of the Earth and has a variable depth, the solution is more complicated since the frequency σ appears in the off-diagonal elements of B as well. If the configuration of the basin is such that we could consider terms of the type:

$$\frac{f}{\sigma h} \frac{\partial \eta}{\partial Y} \frac{\partial h}{\partial X} \quad , \quad \frac{f}{\sigma h} \frac{\partial \eta}{\partial X} \frac{\partial h}{\partial Y} \qquad (4.9.6)$$

as negligible quantities, appearing in (4.6.2), then the eigenvalues of B provide a solution which approximate the problem. On the other hand it is well known that the eigenfrequencies of the basin's gravitational modes are slightly affected by the Coriolis force.

It should be noticed that the low frequency modes caused by the unhomogeneity of the vorticity potential (McConnel 1947), -see for instance the terms in (4.9.6)-, called rotational or quasi-geostrophic modes, are not possible to be derived by such an analysis.

5. NUMERICAL SOLUTION FOR THE AEGEAN BASIN

The above theory is applied on the Aegean sea, having a peculiar shape comparing with other partially closed basins like the Adriatic, Baltic etc. The characteristics of the Aegean have already given in previous paragraphs.
For the numerical solution and further analysis of the hydrodynamic equations, it was necessary to discretize the problem. Using a Mercator map of the Aegean, we constructed two separate grids trying to follow as close as necessary the actual coastal line of the bordering terrestrial line as well as the shape of the islandic blocks, (Fig.14).

5.1. The modeling.

The first grid model was made by dividing the basin in 10x10 prime rectangles (MOD10). Referred to a mean latitude of 38° the ΔX step corresponds to 14.48 km, while the ΔY step corresponds to 18.45 km, on the Earth's surface.
The second grid model was constructed by dividing the basin in 30x30 prime rectangles (MOD30). Referred to the same latitude as above, the ΔX step here corresponds to 43.44 km

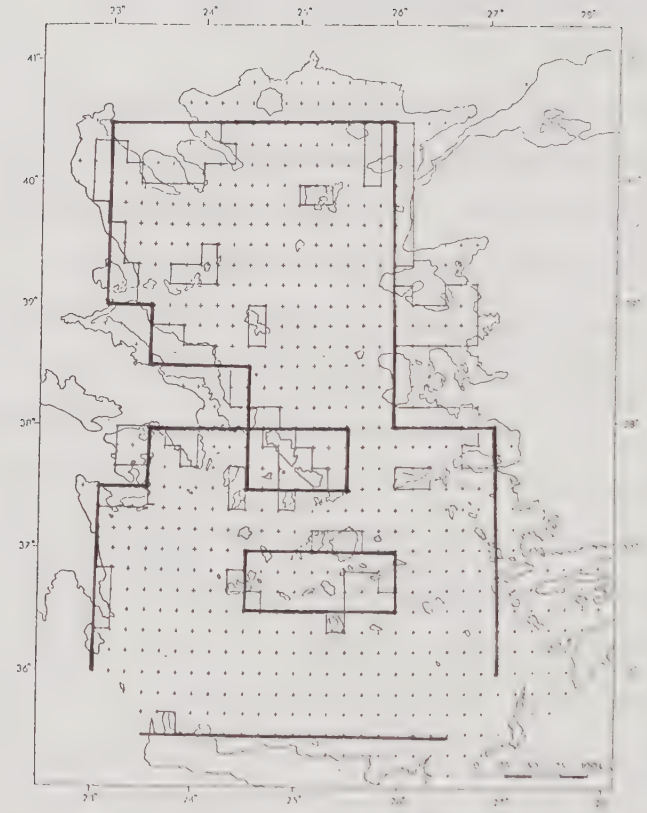

MOD10
MOD30

Fig.14. MOD10 and MOD30.

while the ΔY one corresponds to 55.35 km on the Earth's surface.

The MOD10 was used for the numerical solution thus for the computation of the amplitudes and phases at each sea-point intersection of the grid, while the MOD30 was used for the analysis of the inverse of the corresponding design matrix as well as for the eigen-study of the Aegean basin.

The discretization procedure which was applied to both models, (already described in the previous chapter), follows Forsyte and Wasow 1960 and was successfully tasted on Adriatic, Mediterranean and Baltic basins, (Baxa et al. 1970, Baxa et al. 1973, Bozzi Zadro 1976). The bathymetric data have been derive by interpolating the recent detailed bathymetric map of the Aegean by Morelli et al. 1976.

The number of complex equations were 620 for MOD10, that means a 620x620 design matrix A, while the number of equations for the MOD30 were reduced to 81.

At the W-opening of the basin, we have used as input values the ones available from the existing Adriatic and Mediterranean solutions, while for the E-opening, which is the more important one, values given by Defant 1961 and from the Dodecanesos tidal map given by Tenani 1940.

The system was constrained by the tidal constants derived after the spectral analysis of tidal data from Kavala and Heraklion, (see chapter 3).

As it is clear from the dimensions of the design matrix A, concerning the MOD10, it is difficult to apply direct computing procedures for the solution of the system, -which is actually focused at the inversion of the 620x620 complex matrix-, without applying special computer storage techniques. Recalling the characteristics of the design matrices in our layout, namely the large number of zero elements and the band form of A, it could be possible to apply partitioning inversion or existing subroutines in extensive use for the inversion of large geodetic band matrices, (see for instance the review by Meissl 1975).
Here we have used a fast routine for the solution (inversion) based on the Gaussian decomposition method, (indirect method), developed at the Istituto di Geodesia e Geofisica, University of Trieste, by Dr. L. Bernetti. The routine was runned through a CDC 6400 computer of the University of Trieste.

For the analysis of the MOD30 matrix A, having smaller dimensions we have preferred to use direct processing rou-

tines which could print out the whole inverted design matrix as well as its eigenvalue spectrum. Having the A^{-1} fully printed-out it could be possible to study the tidal impulse responses of points within the basin, varying the input data. From the complete eigenvalue spectrum of A, it could be studied as well the eigenfrequency behaviour of the basin. It is obvious that with these direct routines the gain in information is loose in time, because of the higher computational requirements concerning computer time: The CDC 6600 computer of CINECA, Bologna, gave the answer! For the inversion and the eigenvalue analysis we have used direct routines based on Gauss and Jacobi methods respectively.

5.2. The solution

In order to study in details the response of the basin at semidiurnal tidal frequencies, taking into account the Coriolis force, we have used the MOD10. In this case the major difficulty for the integration of the hydrodynamic equations, -using only the input values at the E and W-openings-, comes from the poor knowledge of the values which

have to be assigned at the natural openings of the basin. Various numerical tests were applied on MOD10 varying everytime the input conditions at the openings, in order to examine the corresponding influence in the tidal dynamics of the Aegean. We have used 5 input points at the W-opening and 4 at the E-opening, (Fig.15).

For adiabatic conditions and assigning every time only one non-zero input test point, (amplitude 1, phase 0), results the following:

i. E-opening, (4 points): The NAB is connected directly to this opening and responds with a maximum amplitude of 40% at the NW Hellenic coast, (Kavala-Thessaloniki), when the input values are applied at the two extreme points of the opening E1 or E4, while the amplitudes are reduced to 20% when operating the two input points E2, E3. The phases of the NAB are varying smoothly and progressively : From 0° at the input, to about -30° at the NW coast for an impulse at E4 and from 0° at the input to about +50° at the NW coast, for an impulse at E1; Using the input points E2 and E3, the phases are almost evanescent within the NAB.

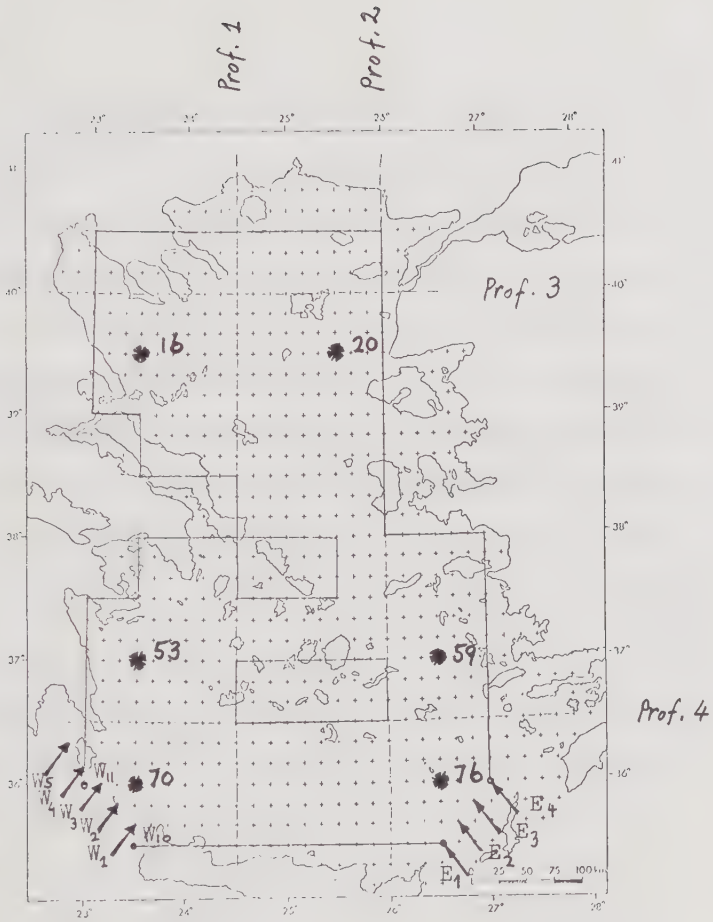

Fig. 15. MOD30; profiles, test impulses.

The SAB actually connected with the Ionian sea, responses weakly to all the four input points of the E-opening: Using the input point E1, we obtain maximum amplitudes of 10%. The phases are smoothly and progressively varying as well. They are negative up to -40° at the area fo the Saronikos gulf, (S of Attica), concerning the input pulse point E4. Moving the input point from E4 to E1, the phases rotate becoming evanescent for E3 and E2, then positive for the input point E1 (20° at the Saronikos gulf and 50° at NNW of Crete).

ii. W-opening, (Kythira- W Crete), 5 points: The NAB responses with an uniform amplitude of 10% when the input point is either W1 or W5 and with amplitudes of 20% at the NW coast, (Thessaloniki area), and of 10% at the southern areas, when using the W2 or W3 input points. The maximum response is noticed when we use the W4 input point, the amplitude being progressively increasing from 10% to 30% following the N direction. In all cases the phase lag between the southern and northern regions of the NAB is of about 60°, moving the input point from W1 to W5, the phases in NAB rotate in such a way that in

the southern area as well as in the northern area result the following phases, with respect to the five input points W1, W2, W3, W4, W5: -35°, 25°; -10°, 50°; 0°, 60°; 15°, 80°; 60°, 120°.

The SAB responses as following: We have a uniform response of 10% for the W1 input point, a 20% response concerning the area between Crete and the Cycladic block and a 10% response at the northern areas for W2 and W3; a 30% and 20% response N and S of the Cycladic block for W4. Finally we obtain 20% and 10% responses N and S of the Cycladic block respectively when operating W5. Moving step by step along the W-opening from W1 to W5, the maximum determined phases at the northern part of SAB, (Saronikos), are respectively: -35°, -10°, -10°, -10°, -40°.

5.3. M2 wave propagation.

The hydrodynamic equations concerning the MOD10, form a complex system of 620 equations. For the solution we have used the following input conditions at the E and W- openings: E-opening: constant amplitude of 5.6 cm and 50°, 60°, 70°, 80° phases for the 4 corresponding input points E4,E3,E2,E1.

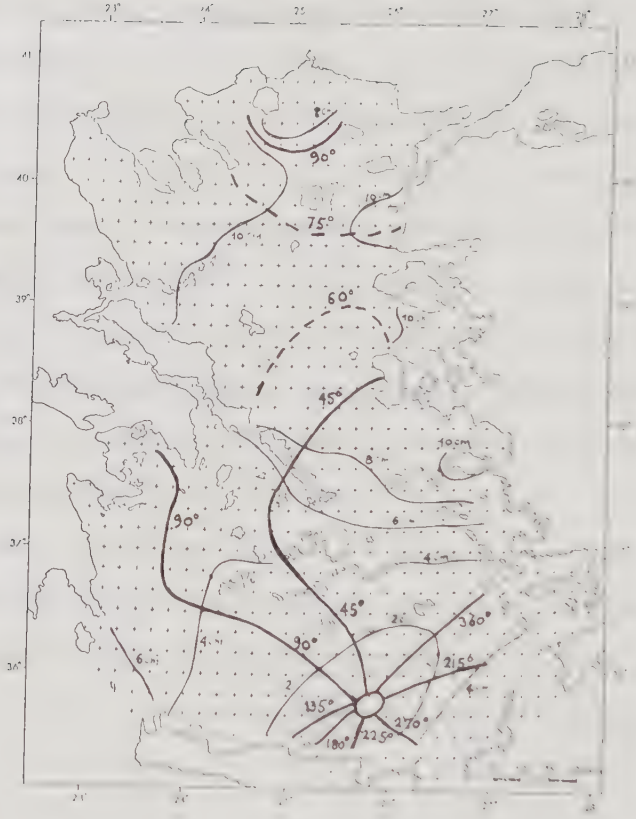

Fig. 16. Aegean sea. M2 wave propagation.

W-opening: constant amplitude of 6.0 cm; constant phase of 260°. In addition to these values at the openings, the solution was constrained by giving the following values at 5 sites of the Aegean basin: Imbros, Leros, Kos, (analysis by Tenani 1940), Kavala, Heraklion, (see previous chapters): 10 cm, 270°; 2.8 cm, 258°; 3.6 cm, 31°; 6 cm, 260°; 2 cm, 138° respectively.

The results are shown in Fig.16.

5.4. The transfer functions.

The transfer functions were calculated along four profiles for 6 different pulse-input points, (Fig.15), taking into account the Coriolis force. The computations were performed by the use of MOD30 thanks to which we obtained the full inverse matrix of the corresponding design matrix A, for input periods varying from 4 to 24 hours with a 4 hours interval. In Fig.17 the transfer functions are given (in scale) for the various cases as functions of the distance from the impulse points and the period.

Following the profiles indicated at Fig.17, we notice the

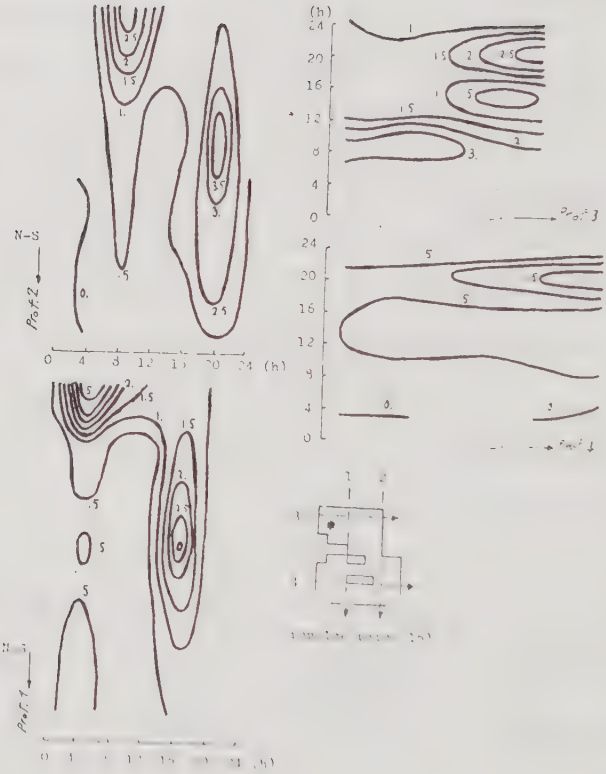

Fig. 17. Transfer function profiles. (see Fig.15).

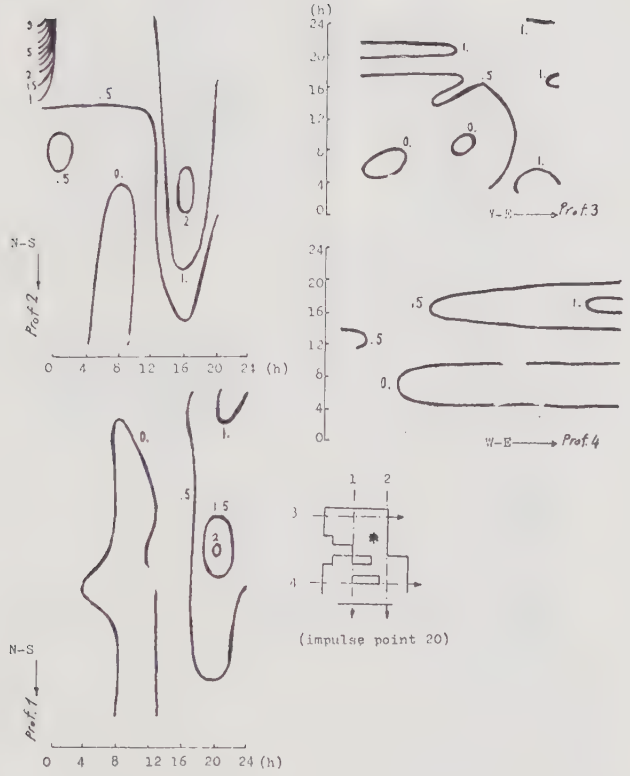
(h)
24
20
16
12
8
4
0
.5
1.
0.
2
W-E
Prof.3
Prof.4
N-S
Prof.2
Prof.1
0 4 8 12 16 20 24 (h)
1 2
3
4
(impulse point 20)

Fig. 17. (cont.)

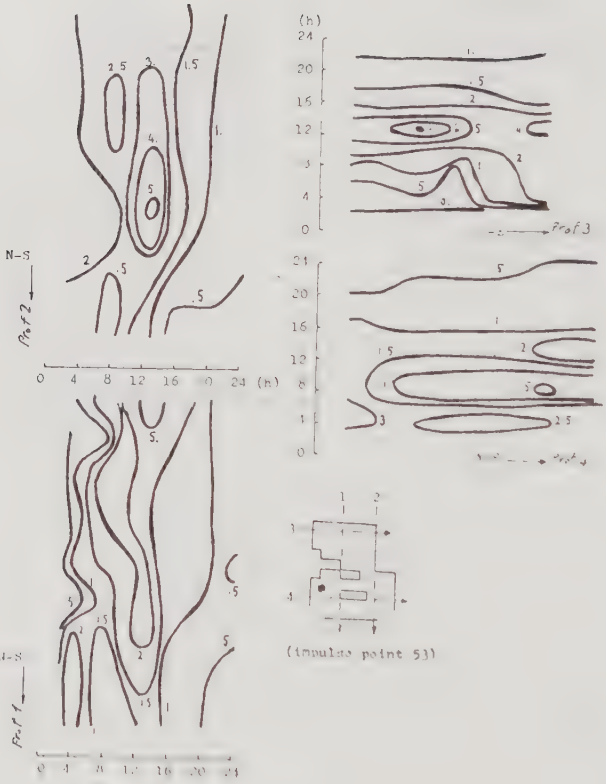
(h)
24
20
16
12
8
4
0
N-S
Prof 2
0 4 8 12 16 20 24 (h)
Prof 3
Prof 1
(impulse point 53)

Fig. 17. (cont.)

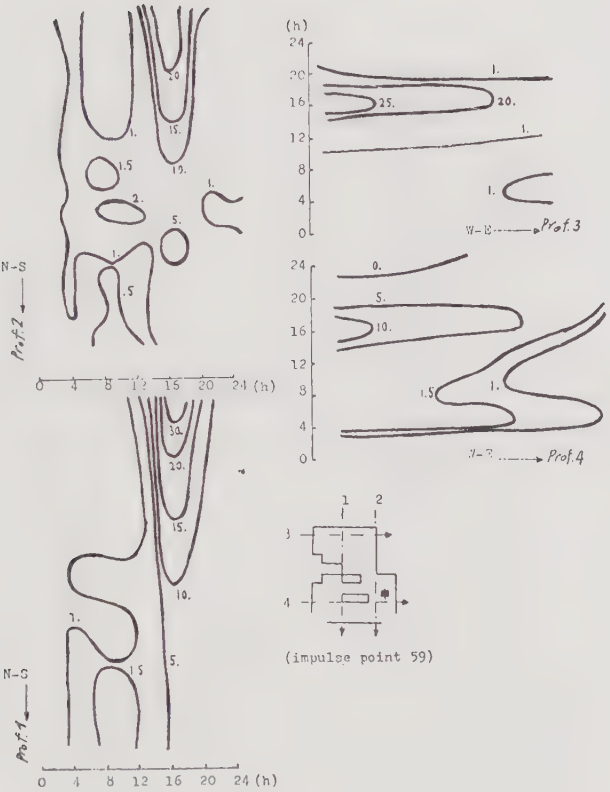
(h)
24
20
16
12
8
4
0
1.
25.
20.
1.
1.
W-E
Prof. 3
0.
5.
10.
1.5
1.
N-S
Prof. 4
1
2
3
4
(impulse point 59)
N-S
Prof. 2
0 4 8 12 16 20 24 (h)
30.
20.
15.
10.
7.
5.
1.5
N-S
Prof. 1
0 4 8 12 16 20 24 (h)

Fig. 17. (cont.)

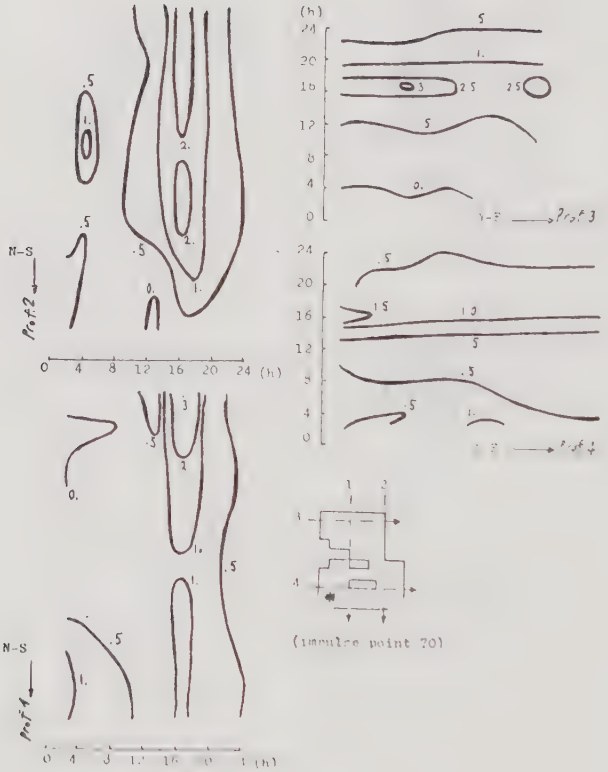

Fig. 17. (cont.)

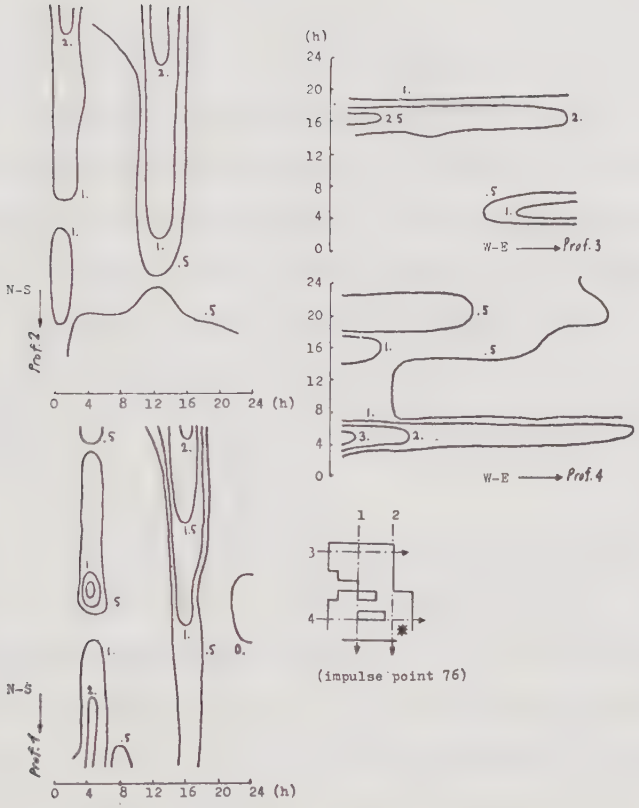
N-S
Prof. 2
0 4 8 12 16 20 24 (h)
N-S
Prof. 1
0 4 8 12 16 20 24 (h)
(h)
W-E
Prof. 3
W-E
Prof. 4
1 2
3
4
(impulse point 76)

Fig. 17. (cont.)

following:

The profile 1 runs half through NAB and half through SAB. In MOD30 the central point corresponds roughly to the channel area which simulates the western passage between the two basins. The profile 2, -S part-, has two points which correspond to the eastern coast of the Cycladic block. The profile 3 runs completely in the northern part of NAB. The profile 4 runs half in SAB and half in NAB; two central points correspond to the southern coast of the Cycladic block.

The numbering of the input points corresponds to the numbering of the grid nodes shown in Fig.14, running from N to S and from W to E; the points 16 and 20 are in the northern NAB, the points 59 and 76 in the southern NAB and the points 53 and 70 in SAB,(see Fig. 15).

5.5. The eigenvalues.

Considering the enlarged A matrix, concerning the MOD30 approach, we have calculated its eigenvalues, without considering the Coriolis force both for an imposed period of

16 hours and for an imposed period of 20 hours. The numerical results obtained in the two cases based on the relation (4.9.5), are in accordance with more than five significant digits: the distinct eigenvalues of the matrix, all negative and real, are 49 and in connection with the eigen-oscillation values of the basin under consideration, between periods of 3 hours nad 20 minutes.
Taking into account the Coriolis force we obtained the eigenperiods of the basin practically the same as before, (values reduced by only 3%).

5.6. Discussion on the results.

The numerical results obtained by MOD10 demonstrate that Defant's hypothesis concerning the independent behaviour of the two basins NAB and SAB, which are almost totally connected with the corresponding E and W-openings of the Aegean, is only partially valid. In fact while the SAB depends a little on the E-opening, the NAB depends in a substancial way on both W and E-openings.
The phases obtained for the various input points along the

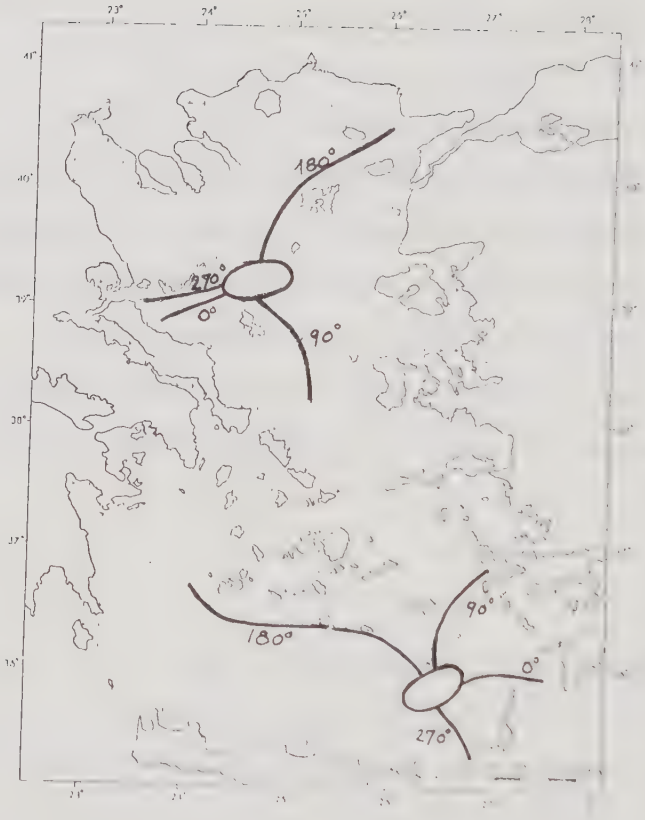

Fig. 18. Test phase-distribution
Case 1.

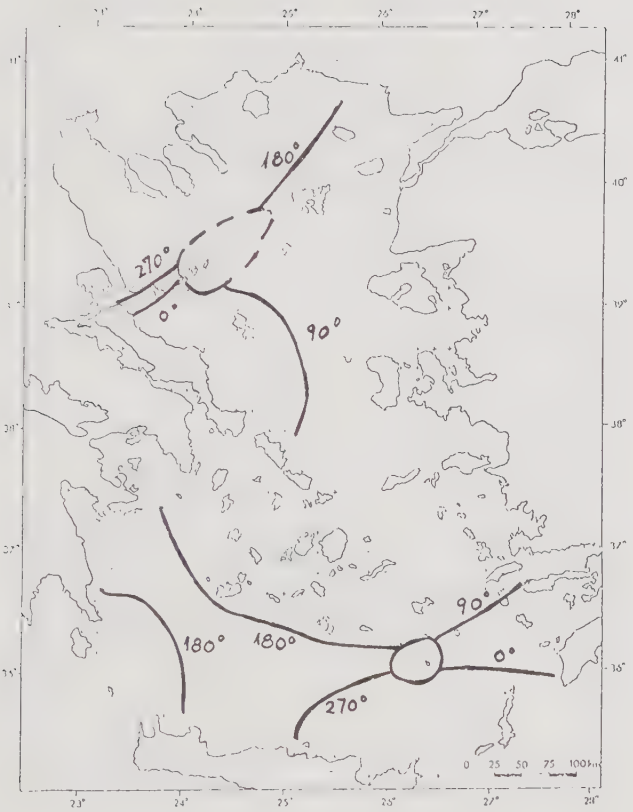

Fig. 19. Test phase-distribution.
Case 2.

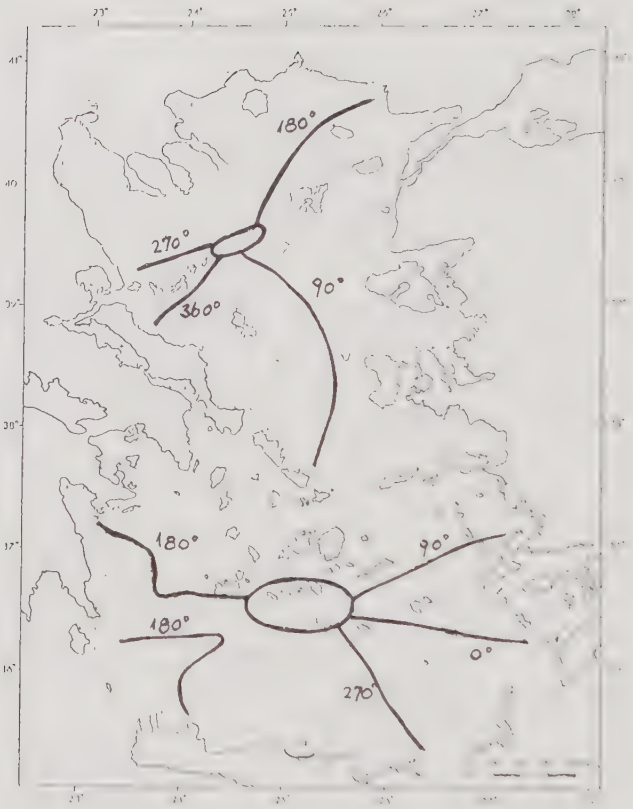

Fig. 20. Test phase-distribution.
Case 3.

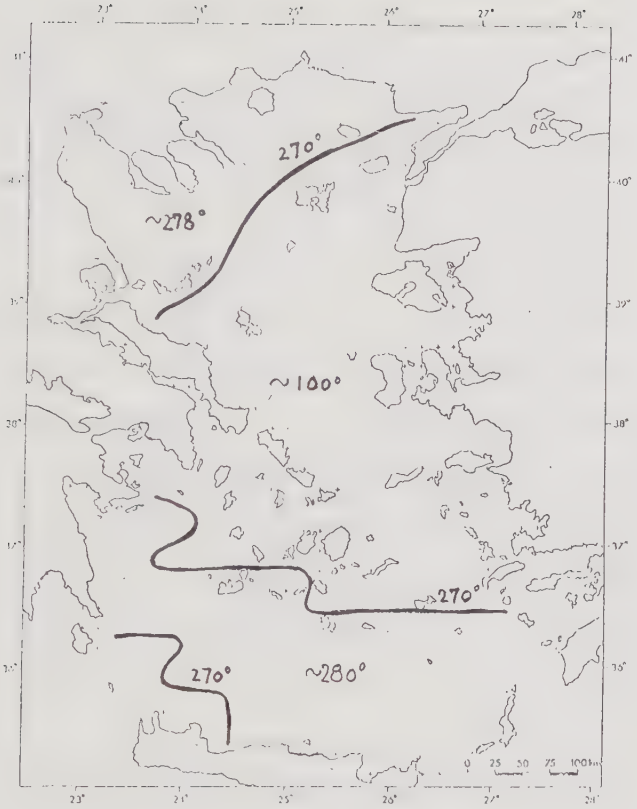

Fig. 21. Test phase-distribution.
Case 4.

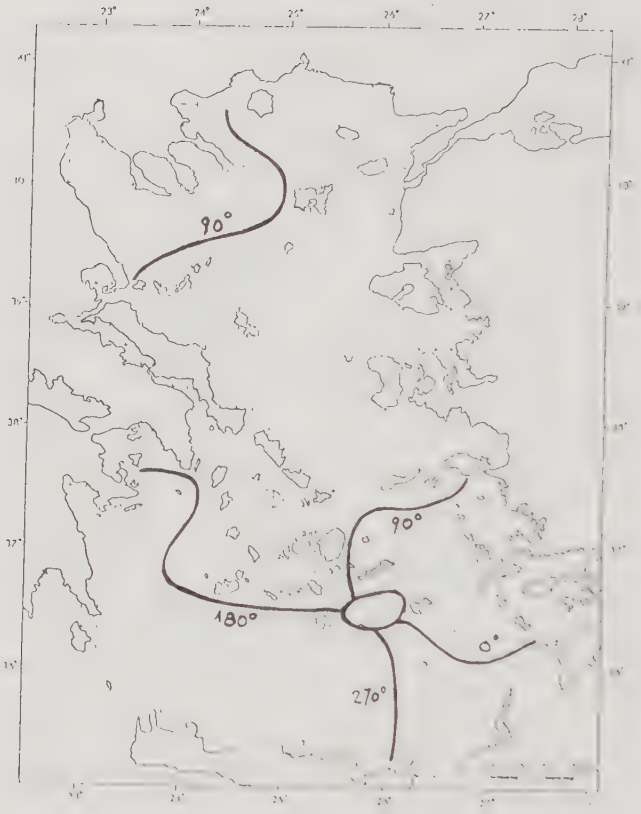

Fig. 22. Test phase-distribution.
Case 5.

two openings demonstrate that the various input points along the two openings demonstrate the formation of an amphidromic node at the SE Cycladic islandic complex area, -which results from the solution for the M2 wave-, is totally dependent on the particular phase conditions, (in practice 180°), between the two openings.

We notice here that numerical results, obtained by varying a little the conditions at the openings and without any value at the coast, indicate the tendency to form one more amphidromic node at the northern part of NAB. This node is developed with minimum of amplitudes to the NE direction, following the proper bathymetry of the region (Fig.4).

The solution obtained, in absence of the Coriolis force, conferms such an hypothesis. For instance : In Fig.18 we solved MOD30 for 12.42 hours period, mean latitude 38°, -that means including Coriolis-, and vanishing the friction; as input values we have used 6.4 cm amplitude and 260° phase for input points W10 and W11. 5.0 cm amplitude and 100° phase for point E1 and 5.0 cm amplitude and 50° phase for point E4, (for the numbering of the input points see Fig.15).

In Fig.19 the MOD30 is solved for the same period, latitude

and friction as above, the same amplitude and phase input values for points W10 and W11, but with 5.0 cm amplitude and 60° phase for both input points E1 and E4.

In Fig.20 with always the same period, latitude and friction we just give 5.0 cm amplitude and 50° phase at the input point E4 and 5 cm amplitude and 80° phase at E1.

In all cases above, appear two nodes: one at the SE corner of the Cycladic complex and the other somewhere at the middle of the NAB. Only at the Fig.20 solution the southern node appears a bit western, around some southern islands of the Cyclades. Comparing all the above cases, we do not observe any significent phase rotation.

In Fig.21 we solve MOD30 for the same 12.42 hours period and zero friction, but without the Coriolis effect, putting the mean latitude equal to zero. The input amplitudes and phases at the points W10, W11 and E1, E4 are the same as in the case of Fig.18.

In Fig.22 the MOD30 is solved using the same values at points W10, W11 and E1, E4 as in the case of Fig.19, keeping 12.42 hours period, 38° latitude and zero friction, but constraining the solution with the already known amplitude, (Tenani 1940), at several coastal sites of the Aegean

e.g. 7 cm for Kavala, 10 cm for Imbros, 2.8 cm for Leros and 3.6 cm for Kos. (For the location of the sites see Fig.8). In this last case there is no node in the northern NAB, but the one close to the Cyclades is still there. Thus we could say, from the analysis above, that probable variations at the openings' input values followed by particular atmospheric conditions, could shape the second node at the northern Aegean.

The computations of the eigenfrequencies of the basin using the MOD30, allows the determination of only gravitational modes. The determined periods, all less than 3 hours, are probably periods of gulf-seiches and of the closed areas of the basin. The solution, even if it could be approximated, obtained without including the Coriolis force which indicates a small reduction of the period with respect to the preceding case, is in accordance with the results obtained by Van Dentzig and Lauwerier 1960 for the case of partially open basins.

Apart of the eigen-oscillations of the gravitational modes it is probable that exists rotational eigen-oscillations having longer periods, caused by the bottom relief of the

basin. Actually the long period oscillations appearing in the analysis of the tidal records of KAV and the maximum of the transfer functions computed for various basin profiles confirm such an hypothesis.

Analyzing the transfer functions at the test-impulse points 16 and 20 (Fig.15), results that the NAB responses in these impulses, mainly at the northern part, for a period of about 20 hours. Strong responses are obtained at the northern coast of the basin for 8 hour periods using the test input point 16, and at the NE coast for 3 to 4 hour periods using the point 20. This last periodicity should correspond to the eigenperiod determined by the eigenvalues of the matrix A: In this case we could inteprete it as the eigen-oscillation of the basin along the NE coast of Thraki.
The SAB responds weakly for all frequencies.
Analyzing the transfer functions of the other two test input points at NAB, 59 and 76, we observe that the NAB and SAB respond, in general, only around 4 hour periods, and for 16 hours. Using the input test point 59 we have a highly amplificated response at the northern parts of NAB, (30 times more the input values), for 16 hours.

The analysis of the transfer function for the two input test points at the SAB allows the conclusion that the two subbasins respond at two frequency bands: The one which corresponds to 12 - 16 hours and the one which corresponds to about 4 hours. The responses are notable at the northern part of NAB when using the test input point 53 for periods at the neighbouhood of 12 to 13 hours,(amplifications of 5 times more the input values).

The whole analysis of the results by using the transfer function method, allows the prediction of what points at the Aegean coast are mostly sensitive to tidal variations as well as to perturbations due to atmospheric effects, in order to organize in a more efficient and feasible way the installation of tidal-gauges for the oceanographic study of the Aegean sea. Such points seem to be: At the extreme E and W, and eventually an intermediate point, of the N cost of NAB; a point on the SE coast of the Peloponnesos and a point at the islands Leros, Kos as well as a couple of points at the Cycladic complex, for monitoring the water flux between the two basins NAB and SAB.

6. THE LOADING EFFECTS

A very interesting geodynamic problem related to the tides is the loading effects, of the sea water movements, applied on terrestrial stations where are in operation instruments, e.g. horizontal pendulums, which could observe the variations of the local vertical, (here the variations -or deflections- of the vertical,have a geodynamic and not the classical geodetic meaning).

These loading effects caused mainly by the sea tides, as well as by the atmospheric pressure, have an indirect character, -compared with the effects of the earth tides, which have a direct character-, and cause a part of the horizontal pendulums and gravity-meters response, namely the effect coming from the local behaviour of the crust, the other part being the effect from the rheological behaviour of the Earth's body connected with the astronomic tides.

Considering the increasing interest for geodynamical studies as part of the scientific activities of the Dionysos Satellite Tracking Station, Athens,we give here a rough estima-

tion of the loading effects, caused by the M2 Aegean tides on the Station.

6.1. On the general theory.

The total loading effect caused by the sea tides is in practice assumed to be proportional to the gravitational effect coming from the solution of the Boussinesq's elastostatic problem. For a detailed solution of this problem concerning an homogeneous semi-infinite solid, see for instance Bozzi Zadro 1966.

The proportionality of the loading effect to the gravitational effect, materilized by a function of the elastic parameters $\varkappa$ and μ of the solid under consideration, where $\varkappa$ the incompresibility modulus and μ the rigidity modulus (for a classical discussion, see Lamb 1917).
This proportionality could be expressed by the coefficient:

$$\alpha = \frac{g^2}{4\pi G} + \frac{3\varkappa + 4\mu}{\mu(3\varkappa + \mu)} \qquad (6.1.1)$$

involving gravity g, and the Newtonian gravitational constant G.

Applying the principle of superposition, (see for instance Bozzi Zadro 1965), the deflection of the vertical, as a function of time, (recall the geodynamic meaning of the deflection of the vertical), called the apparent deflection of the vertical, (a.d.v.), recorded by horizontal pendulums, is a linear combination of the astronomic tide, (a.t.) and of the gravitational effect, (g.e.):

$$(a.d.v.) = (\alpha+1).(g.e.) + \gamma(a.t.) \qquad (6.1.2)$$

where α the coefficient in (6.1.1), γ is a coefficient related with the Love numbers and obviously (a.d.v.), (g.e) and (a.t.) are time functions.

For further discussion on κ and μ values as well as on the coefficients α and γ see for instance Takeuchi 1951 and Marussi 1960.

6.2. M2 loading effects on Dionysos Satellite Tracking Station.

As a contribution to the geodynamical interests of the

Dionysos Satellite Tracking Station, located close to Athens, we have carried out a rough calculation in order to estimate the order of magnitude of the loading effect of the M2 Aegean tides on the station, -having coordinates $\varphi = 38°.079$ N, $\lambda = 23°.933$ E-, for both the N-S and W-E components. Here we have to stress that due to its position the Dionysos station is close to the strait of Euripos, where operates the famous current (see paragraph 2.3), with much higher local tides than the Aegean ones (see for instance Fig.5 and Fig.6). But being this current a totally local phenomenon not influencing the tides within the Aegean basin, and considered as an independent phenomenon for future study, its effects are not included in the present loading estimations.

Using the MOD10 solution for the M2 waves (Fig.16), we have calculated first the Newtonian effect for the amplitude, concerning a cm^2 water area, of the loading points of the Aegean, referred to the Dionysos Station.
In Fig.23 the curves of equal Newtonian effect concerning a cm^2 water area are shown in msec of arc. It is clear that the propagation of the curves are very close related to the $1/r^2$ weight coefficient, where r the distance of the loading

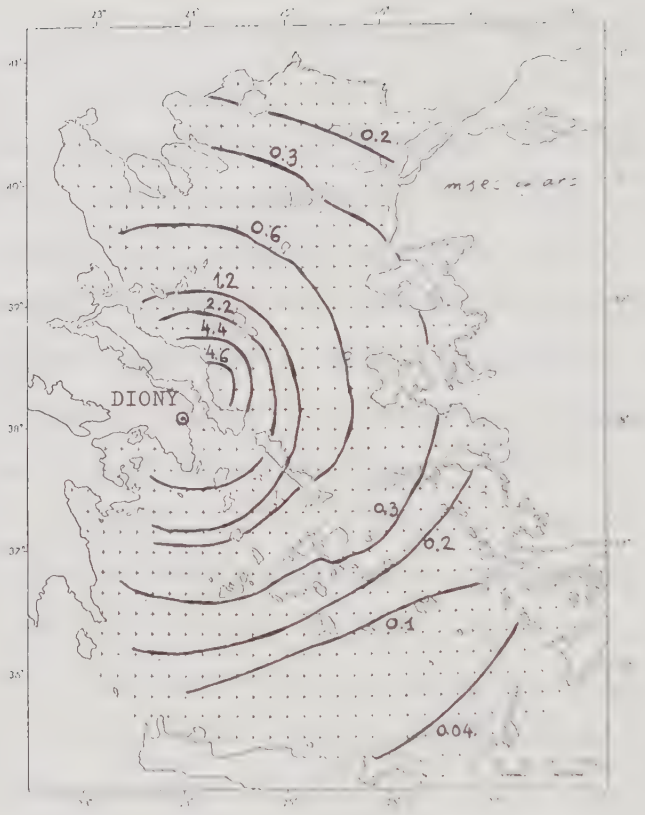

Fig. 23. Distribution of the Newtonian effect for amplitude concerning a cm^2 water area, referred to Dionysos Satellite Tracking Station. (M2 solution). -values X 10^{-12}-.

point of the Aegean from the Dionysos Station. Obviously the Newtonian effect for amplitude concerning a cm^2 water area is too small, recalling the low amplitudes of the Aegean Basin.

For a rough computation of the loading M2 effect on the Dionysos station in both the N-S and E-W components, concering the amplitude and phase, we divided the Aegean basin in 13 blocks using as criterion the distribution of the M2 tides (see Fig.16).

i. For the E-W component at Dionysos we have calculated a Newtonian effect, (N.e), with the following amplitude and phase:

amplitude $(N.e.)_{E-W} = 4.76 \times 10^{-10}$ rad

$= 0.1$ msec of arc

phase : 47.5°

assuming unit water density.

ii. For the N-S component we have calculated for Dionysos the following amplitude and phase:

amplitude $(N.e.)_{S-N} = 1.8 \times 10^{-10}$ rad

$= 0.04$ msec of arc

phase : 79°

From the above order of magnitudes we confirm the a-priori obvious expectations that the Aegean loading effects are too small, due to the low Aegean amplitudes, and even if we multiply (6.2.1) and (6.2.2) by an elastic coefficient of an order of magnitude of 5, (as estimated for instance at Trieste, Bozzi Zadro 1966), we obtain 0.5 msec of arc for the E-W component and 0.2 msec of arc for the S-N component.

CONCLUSIONS AND PROPOSALS

Extensive discussion on the results is given within the specific chapters of the text especially in chapter 5, paragraph 5.6, concerning the semidiurnal solution as well as concerning the transfer functions of the Aegean basin. A long discussion on the spectral analysis of the tidal registrations of KAV and HER are also given in detail in chapter 3, paragraph 3.4.

From the special case of the Aegean sea, we have seen that the descretization of the solution is a very important aspect. It should be selected a well designed grid for the solution following as necessary as possible the actual boundaries of the basin, but thinking always the capacity of the computer where we are going to solve the system of the hydrodynamic equations. A big discussion concerns the computer solution when we have to deal with such big dimension matrices. The problem is focused on the inversion of the design matrix, which we wish to have fully printed-out in order to study the transfer functions of the basin.

The study of the transfer function is an important tool because using them we can estimate the response of the basin to eventual changes of the input harmonic constants which constrain the solution. That means that we could examine the sensitivity of the basin for variations at the openings of the basin as well as for meteorological influences on the tidal behaviour.

From this analysis we could also organize a feasible tide-monitoring project for the Aegean sea, establishing a network of tide recording instruments, by putting them at the appropriate sites and not at places where the tidal response is not significant. Here we must stress the different need for tidal data in navigation and oceanography when organizing a tidal campaign.

A future solution of the hydrodynamical equations for the Aegean basin is suggested after having analyzed more tidal records, preferable from new tidal stations which fit better our needs. These stations should be established in specially constracted tidal wells. The use of some pressure type bottom tide recorders should be suggested.

The application of the programming techniques, concerning the inversion of large matrices already in use in computational Geodesy, could give valuable tools for solving large systems of hydrodynamic equations with the possibility to obtain at the same time the full print-out of the inverse. But there is no doubts that we should always use rather large computers.

From the point of view of the loading effects the influence from the Aegean tides is almost negligible. Special studies have to be done concerning the mostly interesting current of Euripos which consists a special case, not influencing the total Aegean tides, but with a probable higher loading contribution especially on coastal points lying close to the stait where the current runs.

As far as the Dionysos Satellite Tracking station is concerned for a future installation of earth tidal instruments, apart the probable indirect loading effects coming from the Euripos current, the whole Aegean sea is not influencing almost at all the site.

This work is considered as the first condribution within a more general tidal project planned at the Surveying Laboratory of the N.T. University of Athens concerning this very interesting part of our geosciences, giving the "know how" and a first complete M2 tidal map for the Aegean sea, as well as a detailed sensitivity study concerning local impulse effects.

References

BAXA, P., BOZZI ZADRO, M. and TREVISAN, L. (1971): Adriatic Tides in the frequency domain. Proc. Int. Col. Phys. of the Seas, Trieste.

BAXA, P., BERNETTI, L., BOZZI ZADRO, M. and GALMONTE, C. (1973): Numerical solution of the hydrodynamic equations for the Mediterranean basin. VII Symp. Earth Tides, Sopron.

BLACKMANN, R.B. and TUKEY, J.W. (1958): The measurement of power spectra from the point of view of communication engineering. Dover, N. York.

BOGDANOV, K.T. and MAGARIK, V.A. (1967): Solution numerique du probleme de la propagation des ondes de Marees semi-diurnes (M2 et S2) dans l'ocean mondial. Dok. Akad. Naouk SSSR, Tom. 172.

BOZZI ZADRO, M. (1965): On the frequency dependance of the loading effects due to ocean tides and seiches. Comm. No.236, Obs. R. Belg.

BOZZI ZADRO, M. (1966):Maree terrestri ed effeti di carico.
Boll. Geof. Teor. Appl.,Vol. VIII, No.3

BOZZI ZADRO, M. (1970): Spectral Analysis of time serie
ICEE, Intrn. course, UNESCO/CNR, Triest

BOZZI ZADRO, M. and PORETTI, G. (1971):Analisi degli spettri complessi delle maree marine registrate a Trieste
Geof. e Meteo. Vol.XX, No.3/4

BOZZI ZADRO, M. and PORETTI, G. (1972): Spectral Techniques for the Analysis of Tidal Time Series.
Pure and Appl. Geoph. Vol.95.

BOZZI ZADRO, M. (1976): Numerical Solution of the Hydro dynamical equations for the Baltic sea.
(unpublished material).

CARTWRIGHT, D.E. and CATTON, D.B. (1963):On the Fourier analysis of tidal observations.
IHR, Vol. XL, No. 1.

CHRISTENSEN, Jr.N. and GROVES, G. (1970): Toward evaluation of planetary seiches by numarical techniques.
Rep. 70-9, Hawai Inst. Geoph.

CHRISTENSEN, Jr.N. (1972): Numerical simulation of free oscillations of enclosed basins on a rotating earth.
Rep. 72-9; Hawai Inst. Geoph.

COOLEY, J.W. and TUKEY, J.W. (1965): An algorythm for the machine calculation of complex Fourier series. Math. of Comp. 19,No.20.

DEFANT, A. (1961): Physical Oceanography. Vol. I and II, Pergamon.

FORSYTHE, G. and WASOW, W. (1960):Finite-difference methods for partial differential equations. Wiley.

GODIN, G. (1972): The analysis of tides. Liverpool Univ. Press.

HANSEN, W. (1940):Ein Verfahren zur Berechmung der eintägigen tiden. Ann. Hydr. 68.

HANSEN, W. (1943):Ermittlung der Geseiten in beliebig geformten Maresgebieten unter Benutzung der Raudverte. Ann.Hydr. 71.

HANSEN, W. (1948):Die Ermittlung ger Gezeiten beliebig gestalterer Meeresgebiete mit Hilfe des Randwertverfahres. D.Hydr: Zeit, Band I.

HENDERSHOTT, M. and MUNK, W. (1970): Tides. Ann.Rev.Fluid.Mech., 2

HENDERSHOTT, M. (1973): Ocean tides. Trsn. Amer. Geoph. Union.

LAMB, H. (1917):On the deflection of the vertical by tidal loading of the Earth's surface.

Proc. Royal Soc. Vol.93.

LAMB, H. (1932): Hydrodynamics. Cambridge Univ. Pr.

LA PORTE, M. et VIGNES, J. (1974): Methode numerique de detection de la singularite d' une matrice. Numer. Math. 23.

MARUSSI, A. (1961): I primi risultati ottenuti nella stazione per lo studio delle maree della verticale della Grota Gigante. Boll. Geod. Sc. Aff. No.4.

McCONNEL, A.J. (1947): Applications of absolute differential calculus. Blackie & son.

MEISSL, P. (1975): Report of SSG 4:38 of IAG: Computer Techniques in Geodesy. Mitt. Geod. Inst. T.U. Graz; fogle 20.

MORELLI, C., PISANI, M. and CANTAR, C. (1975): Geophysical studies in the Aegean sea and in the eastern Mediterranean. Boll. Geof. Teor. ed Appl.

MURRAY, M. T. (1964): Optimization processes in tidal analysis. IHR Vol.XLII, No.1.

PLATZMAN, G. (1972): Two dimensional free oscillations in normal basins. J. Phys. Ocean. Vol.2, 2.

PLATZMAN, G. (1975): Normal modes of the Atlantic and Indian oceans. J. Phys. Ocean. Vol.5, 2.

SHUREMAN, P. (1958): Manual of harmonic analysis and prediction of tides. USCGS, Sp. Publ. 98.

TAKEUCHI, H.,I. (1951): Fac. Sci. Univ. Tokyo Sect II 7, Part II, 1.

TENANI, M. (1930):Sur les marees della Mediterrané orientale. Comp. rend. 21 Jul. 1930.

TENANI, M. (1940):Maree e correnti di marea. I. Idr. R. Mar., Genova.

VAN DANTZING D. (1958):Solutions of the equation of Helmoltz in an angle with vanishing directional derivatives along each site. Rep. TW 51, Math. Cent. Amsterdam.

VAN DANTZING, D. and LAUWERIER, A.H. (1960): The north sea problem IV, free oscillations of a rotating rectangular sea. Proc. Ser.A.63,No.4., Indag. Math.22, 4.

VARIANGHIN, M. (1972): Tides and Tidal values for hellenic ports. Ocean.St. 9, Hydr.S. Hell. Navy, (in greek).

VEIS, G. (1954):Tables for the calculation of the tidal current of Euripos.(unpublished).

WILKINSON, J.H. (1960):Error analysis of floating point computation. Numer. Math. 2.

WILKINSON, J.H. (1963): Rounding errors in algebraic process. Prentice Hall.

Curriculum vitae

1970 : Dipl. Eng., National Technical University, (NTU), Athens, Greece.

1971 up to day : Assistant at the NTU.(Prof. G. Veis).

1972 (summer) : At Smithsonian Astrophysical Observatory, (SAO), Cambridge, Ma., USA. Fellowship: Smithsonian Institution.

1973 (summer) : At SAO, Cambridge, Ma., USA.

1974 : Dr. Eng., NTU, Athens, Greece.

1975 (Jan/Dec) : At the Geodetic Institute, Uppsala University (UU), Sweden.(Prof. E. Tengström). Grants from NTU and UU.

1976 (Jan/Jun) : At the Institute of Geodesy and Geophysics, University of Trieste, Italy.(Prof. A.Marussi, Prof. M. Zadro). Fellowship: Commissione Geodetica Italiana.

1976 (Jul/Dec) : Fellowship: Alexander von Humboldt-Stiftung, for rsearch at Munich, F.R. Germany. (Prof. E. Grafarend).